

QC852
.C6
no. 491
ATSL

**PARAMETERIZATION OF
CLOUD MICROPHYSICAL PROCESSES
IN THE CSU GENERAL CIRCULATION MODEL**

Laura D. Smith and David A. Randall

Department of Atmospheric Science
Colorado State University
Fort Collins, CO 80523

February 1992

**Colorado
State
University**

**DEPARTMENT OF
ATMOSPHERIC SCIENCE**

PAPER NO.

491

QC852
.C6
no. 491
ATSL

Parameterization of Cloud Microphysical Processes in the CSU General Circulation Model

Laura D. Smith and David A. Randall

*Department of Atmospheric Sciences,
Colorado State University,
Fort Collins, Co 80523*

February 1992

Abstract

The chief microphysical processes required to simulate the formation and dissipation of cloudiness have been implemented in the CSU general circulation model (GCM) with the aim to (1) yield a more physically-based representation of the sources and sinks of the atmospheric moisture components, (2) link the fractional cover and optical properties of model-generated clouds to predicted liquid/ice water amounts; and (3) produce more realistic temporal behaviors of the cloud fields. The bulk microphysics scheme encompasses five prognostic variables of water vapor, cloud water, cloud ice, rain, and snow. Cloud liquid and ice water amounts are predicted to form through large-scale condensation and sublimation processes plus detrainment at the top of convective cumulus towers. The instantaneous production of rain and snow is obtained through autoconversion of liquid water droplets and ice crystals. The growth process of rain drops and snow flakes falling through the free atmosphere is simulated using the continuous collection equation. Evaporation of cloud liquid, cloud ice, rain, and snow occurs in subsaturated layers. Melting and freezing are also taken into account. This document gives a description of the cloud microphysics package and its implementation into the CSU GCM.

Contents

1	INTRODUCTION	6
2	THE CLOUD MODEL	11
2.1	General description	11
2.2	Model flow	13
3	CLOUD MICROPHYSICS	17
3.1	Rain and snow size distributions	17
3.2	Mass-weighted fallspeeds	17
3.3	Sources and sinks of the water continuity variables	18
3.3.1	Condensation of water vapor/Evaporation of cloud water (PCOND)	18
3.3.2	Autoconversion of cloud water (PRAUT)	20
3.3.3	Collection of cloud water by rain water (PRACW)	20
3.3.4	Evaporation of rain water (PREVP)	21
3.3.5	Sublimation of water vapor/Evaporation of cloud ice (PSUB)	22
3.3.6	Autconversion of cloud ice to snow (PSAUT)	22
3.3.7	Collection of cloud ice by snow (PSACI)	23
3.3.8	Collection of cloud water by snow (PSACW)	23
3.3.9	Depositional growth of snow (PSEVP)	23
3.3.10	Melting of snow (PSMLT)	24
3.3.11	Melting of cloud ice (PSMLTI)	25
3.4	Source terms for the water continuity variables	25
3.5	Conservation of the generalized moist static energy	26
4	TEST OF EACH PROCESS	27
4.1	Process PCOND	27
4.1.1	Condensation of water vapor	27
4.1.2	Evaporation of cloud water	28
4.2	Process PRAUT	29
4.3	Process RWFALL	30
4.4	Process PRACW	30
4.5	Process PREVP	31
4.6	Process PSUB	32
4.6.1	Sublimation of water vapor	32
4.6.2	Evaporation of cloud ice	38
4.7	Process PSAUT	39
4.8	Process SNFALL	40
4.9	Process PSACI	40
4.10	Process PSACW	42
4.10.1	Accretion of cloud water by snow	42
4.10.2	Accretion of cloud water by melting snow	42
4.11	Process PSEVP	43
4.12	Process PSMLT	44
4.13	Process PSMLTI	45
A	LIST OF SYMBOLS	55
A.1	Symbols in Section 3	55
A.2	Symbols in Section 4	58

List of Figures

1	Schematic illustration of the interactions between cloud microphysical processes, and convective and radiative processes.	7
2	Schematic illustration of the cloud microphysics processes.	15
3	Schematic illustration of the model flow.	16
4	Mass-weighted mean terminal velocity for rain and snow at prescribed pressure levels. The four top curves are for rain. The four bottom curves are for snow.	19
5	<u>Process PRAUT</u> - Increase of (a) the cloud water mixing ratio, (b) the rain mixing ratio, and (c) the temperature when supersaturation occurs and rain starts to form by auto-conversion of cloud water droplets.	33
5	<u>Process PRAUT-continued</u>	34
6	<u>Process RWFALL</u> - Falling of rain.	34
7	<u>Process PRACW</u> - (a) Decrease of the cloud water mixing ratio by accretion of rain, and (b corresponding increase of the rain mixing ratio in layers for which ($T \geq 0^\circ\text{C}$)).	35
8	<u>Process PREVP</u> - (a) Increase of the relative humidity, (b) decrease of the rain mixing ratio, and (c) decrease of the air temperature due to evaporation cooling.	36
8	<u>Process PREVP-continued</u>	37
9	<u>Process PSAUT</u> - Increase of (a) the cloud ice mixing ratio, (b) the snow mixing ratio, and (c) the temperature when supersaturation occurs and snow starts to form by auto-conversion of cloud ice crystals.	47
9	<u>Process PSAUT-continued</u>	48
10	<u>Process SNFALL</u> : Falling of snow.	48
11	<u>Process PSACI</u> - (a) Decrease of the cloud ice mixing ratio by accretion of snow, and (b) corresponding increase of the snow mixing ratio in layers for which ($T < 0^\circ\text{C}$).	49
12	<u>Process PSEVP</u> - (a) Increase of the relative humidity, (b) decrease of the snow mixing ratio, and (c) decrease of the air temperature due to evaporation cooling.	50
12	<u>Process PSEVP-continued</u>	51
13	<u>Process PSMLT</u> - (a) Decrease of the snow mixing ratio, and (b) corresponding increase of the rain mixing ratio.	52

List of Tables

1	Status of parameterization of cloud water content and precipitation used in GCMs. Symbols are given in Appendix A.	9
1	<i>continued.</i>	10
2	Keys to Fig. 2	11
3	pcond: p=953.5mb - t=60s	27
4	pcond: p=953.5mb - t=60s	28
5	praut: p=958.5mb - t=60s	29
6	rwfall: t=60s	30
7	pracw: p=958.5 mb - t=60 s	30
8	prevp: p=958.5mb - t=60s.	31
9	psub: p=230mb - t=60s	32
10	psub: p=230mb - t=60s	38
11	psaut: p=230mb - t=60s	39
12	snfall: t=60s	40
13	psaci: p=230mb - t=60s	41
14	psacw: p=525.5mb - t=60s	42
15	psacw: p=596mb - t=60s	43
16	psevp: p=230mb - t=60s	44
17	psmlt: p=596mb - t=60s	45
18	psmlti: p=596mb - t=60s	46

Acknowledgments

This research was sponsored by the National Science Foundation under the grant ATM-8907414.

1 INTRODUCTION

One current challenge in the development of atmospheric general circulation models (GCMs) deals with the parameterization of the various components of the atmospheric hydrologic cycle and their interactions with the other components of the model physics.

The complexity to reproduce the different interactions between the cloud water parameters and the model physics is best illustrated in Fig.1. The driving variables of the hydrologic cycle are the cloud liquid (ice) water contents. Condensation (sublimation) from large-scale and convective processes is the chief source of cloud liquid (ice) water. Cloud water may be removed from the atmosphere in the form of precipitation or may evaporate. Cloud water interacts with convection by turbulent mixing and, vice versa, convective systems may act as sources of liquid (ice) water by detrainment at the top of convective columns. Aside from the specific process of formation/removal of cloud water, there also exist mutual interactions between the rates of condensation, evaporation, and precipitation, and the convective circulations. Once cloud water is predicted to form, it directly affects the distribution of cloudiness and its optical properties. It is obvious that the horizontal cloud fraction depends upon the cloud water content. Also, it is strongly dependent upon the intensity of convection. Finally, cloud water interacts with radiation by modifying the optical thickness and infrared emissivity of clouds.

At present, several GCMs include a prognostic equation for the mass of liquid and frozen water, as well as an explicit description of the conversion rate of cloud liquid/ice water to precipitation. Table 1 gives a list of various studies and their treatment of each component of the problem—diagram shown in Fig. 1. Two classes of parameterizations may be distinguished.

The first class (Del Genio and Yao, 1990; Le Treut and Li, 1991; Roeckner *et al.*, 1990; Smith, 1990) is based on the approach of Sundqvist (1978) and Sundqvist *et al.* (1989) on parameterizing large-scale condensation cloud water content and associated cloudiness. Sundqvist (1978) and Sundqvist *et al.* (1989) simultaneously solve the equations for the rate of change of the liquid water content and fractional cloud amount. Condensation is predicted to start if the relative humidity exceeds a threshold relative humidity, hence allowing for sub-grid scale cloud cover. The

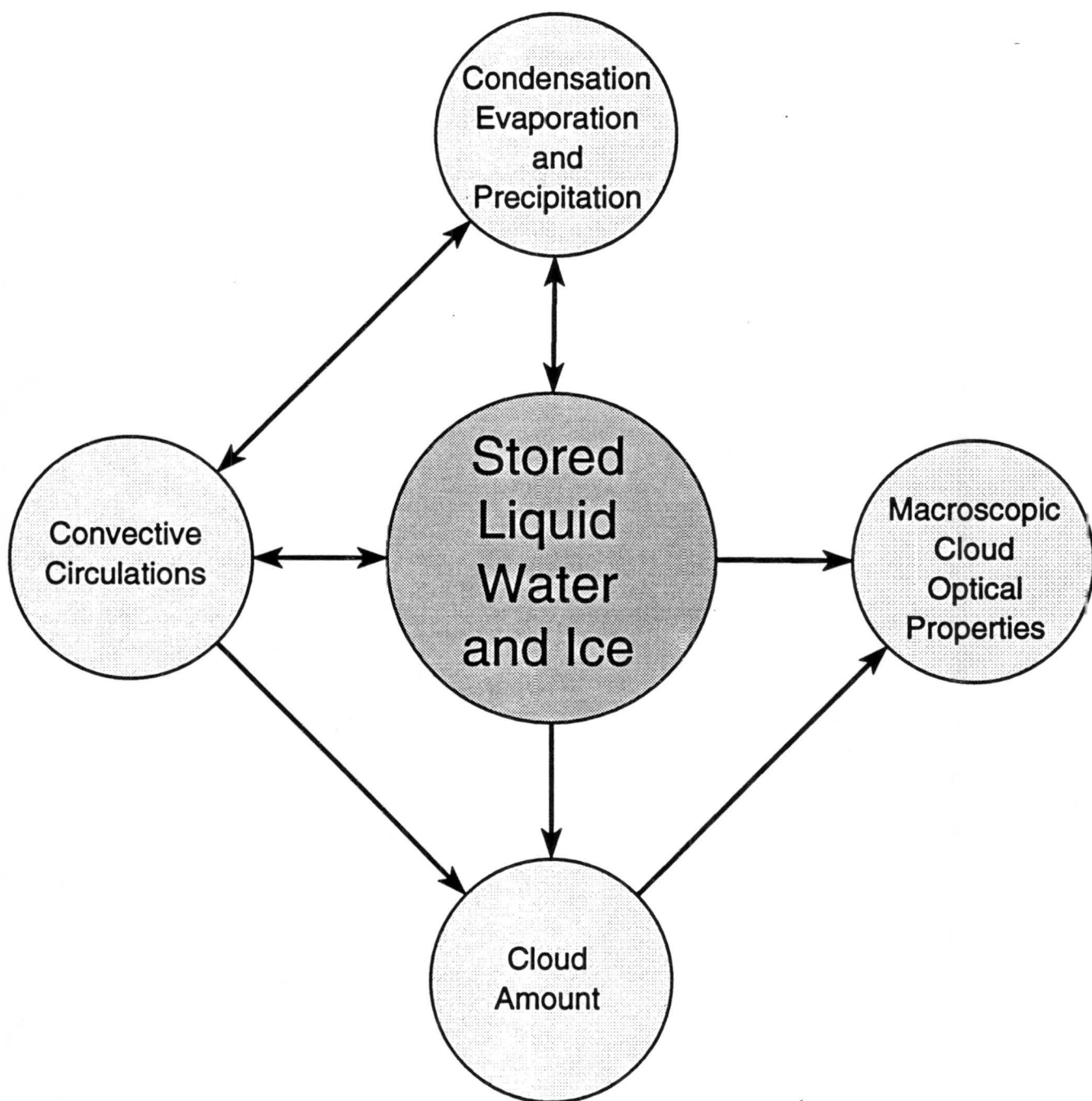


Figure 1: Schematic illustration of the interactions between cloud microphysical processes, and convective and radiative processes.

condensation rate depends upon the relative humidity and moisture flux convergence. The relation employed for the rainfall rate qualitatively accounts for the autoconversion of cloud droplets to rain drops and accretion of cloud water by rain, as discussed by Kessler (1969). The prediction scheme for cloud water and fractional cloudiness implemented in the GISS (Del Genio and Yao, 1990) and the ECHAM (Roeckner *et al.*, 1990) GCMs follows very closely that of Sundqvist (1978) and Sundqvist *et al.* (1989). Smith (1990) computes the cloud amount and cloud water content using the cloud distribution concept developed by Sommeria and Deardoff (1977) and Mellor (1977). A statistical distribution of the moist conservative variables about their grid-box mean is assumed. Finally, Le Treut and Li (1991) derives the fraction of the grid where condensation occurs by assuming a “top-hat” distribution of the total (vapor plus liquid) water content. The parameterization of the precipitation is highly simplified and is based on the assumption that all the cloud water in excess of a prescribed threshold is instantaneously removed from the atmosphere in the form of rain.

The second class of GCMs (Ghan and Easter, 1991; Ose, 1991) uses modified versions of bulk cloud microphysics parameterizations that were originally developed for cloud mesoscale models. Ghan and Easter (1991) test the Colorado State University (CSU-RAMS) cloud microphysics package (Cotton *et al.*, 1982, 1986; Flatau *et al.*, 1989) for running conditions suitable for GCMs. Difficulties which may result from differences in the temporal and spatial resolution of a large-scale versus mesoscale model are emphasized. In particular, Ghan and Easter (1991) shows that the inclusion of a “diagnostic” versus “predicted” equation for the precipitation species, and instantaneous melting, allows the use of longer time-step without significantly affecting the model performance to simulate the time evolution of the cloud liquid and ice variables.

Ose (1991) includes two prognostic variables of the cloud liquid and cloud ice water amounts and simple microphysics processes to the UCLA GCM to study the life-cycle and radiative properties of cirrus clouds. Autoconversion of cloud liquid droplets (cloud ice crystals) to rain drops (snow flakes), accretion of liquid droplets (ice crystals) by rain (snow), evaporation, melting, and freezing processes of precipitation and cloud water are incorporated in a simple manner.

In this report, we describe the bulk cloud microphysics parameterization scheme which has been implemented in the Colorado State University GCM (CSU GCM). In section 2, the different

interactions between water vapor, cloud water, cloud ice, rain, and snow are described. Also the model flow, as is presently coded in the CSU GCM, is outlined. The bulk equations of the microphysics parameterization scheme are given in section 3 while results of simple tests run for each microphysical process are summarized in section 4.

Table 1: Status of parameterization of cloud water content and precipitation used in GCMs. Symbols are given in Appendix A.

STUDY	CONDENSATION, PRECIPITATION, EVAPORATION	CLOUD FRACTION	OPTICAL PROPERTIES
Del Genio and Yao (1990)	q_c and q_i from large-scale condensation plus moist convection. Probability function for liquid or ice formation. Follow Sundqvist (1978) for E_r and P_r .	As in Sundqvist (1988).	As in Stephens (1978).
Le Treut and Li (1991)	q_c from large-scale condensation, moist convection, plus Kuo-type convective scheme. P_r depends upon a threshold value of q_c for warm clouds, and q_v and T for cold clouds ($T < -10^\circ\text{C}$).	Equal to 100% or to the surface fraction of active cumulus for convective clouds. Simple statistical scheme for stratiform clouds.	As in Stephens (1978).
Ghan and Easter (1991)	CSU bulk cloud microphysical scheme. Precipitation species are diagnostic rather than prognostic quantities.	Not included.	Not included.
Ose (1991)	q_c , q_i , P_r , and E_r from a simple bulk microphysics scheme. q_c and q_i from large-scale condensation plus detrainment from cumuli.	Limited to two values, 0. or 1.	As in Stephens (1978) for water clouds. As in Liou et al. (1978) and Starr et al. (1985) for ice clouds.
Roeckner et al. (1991)	q_c and q_i from large-scale condensation plus moisture flux convergence (Sundqvist, 1978). The partition between q_c and q_i is empirical, based on Rockel (1988). Follow Sundqvist (1978) for E_r , and P_r for the liquid phase. Follow Heymsfield (1977) for P_r for precipitation of ice.	As in Sundqvist (1988).	As in Stephens (1978).
Smith (1990)	Cloud water from statistical distribution about the grid-box mean. The partition between q_c and q_i is given by a quadratic spline. P_r adapted from Goldin (1986). E_r proportional to the sub-saturation.	Assumes a statistical distribution about the grid-box mean.	Prescribed.
Sundqvist (1978)	Liquid phase only. q_c from large-scale condensation plus moisture flux convergence. P_r proportional to cloud water mass and typical conversion time of cloud droplets to rain drops. E_r proportional to the subsaturation.	From a prescribed relative humidity threshold.	Not included.

Table 1: *continued.*

STUDY	CONVECTIVE PROCESSES	LARGE-SCALE ADVECTION	NUMERICAL ASPECTS
Del Genio and Yao (1990)	Mixing at cloud-top, Randall (1980).	No	Not specified.
Ghan and Easter (1991)	Not specified	Not specified	Upstream scheme for vertical advection and fallout. Impact of model time-step.
Le Treut and Li (1991)	No interactions.	Yes	Not specified.
Ose (1991)	Detrainment from cumuli.	No	Not specified.
Roeckner et al. (1991)	No interactions.	Yes	Not specified.
Smith (1990)	Turbulent mixing in cloudy regions.	No	Not specified.
Sundqvist (1978)	No interactions.	Yes	Not specified.

2 THE CLOUD MODEL

2.1 General description

The model structure is largely based upon that described in Lin et al. (1983), and Rutledge and Hobbs (1983). Five prognostic variables for the mass of water vapor, cloud water, cloud ice, rain, and snow, are taken account. It is assumed that the terminal fall velocity of cloud liquid/ice water particles may be neglected compared with the velocity of air, rain, and snow. Rain and snow are assumed to have non negligible fall velocities. Figure 2 depicts the interactions among the five species which have been included in the cloud microphysics package and explained in Table 2. Each microphysical process is highly parameterized and explained in the next section.

Table 2: Keys to Fig. 2

Symbol	Meaning
PCOND	Condensation of water vapor to cloud water/ Evaporation of cloud water to water vapor.
PRAUT	Autoconversion of cloud water to rain.
PRACW	Collection of cloud droplets by rain.
PREVP	Evaporation of rain.
PSUB	Sublimation of water vapor to cloud ice/ Evaporation of cloud ice to water vapor.
PSAUT	Autoconversion of cloud ice to snow.
PSACI	Collection of cloud ice crystals by snow.
PSACW	Collection of cloud water by snow; produces snow if $T < T_0$ or rain if $T \geq T_0$. Also enhances snow melting for $T \geq T_0$.
PSEVP	Evaporation of snow.
PSMLTI	Melting of cloud ice to form cloud water, $T \geq T_0$ / Freezing of cloud water to form cloud ice, $T < T_0$.
PSMLT	Melting of snow of to form rain, $T \geq T_0$.

Interactions between water vapor, cloud water, cloud ice, rain, and snow, and differences between the present cloud microphysics package, and Lin et al. (1983) and Rutledge and Hobbs (1983), may be summarized as follows:

Water vapor as a source: Water vapor is a source of both cloud liquid and cloud ice water through instantaneous processes. Cloud liquid water is predicted to form by condensation of vapor when the temperature (T) is equal or greater than 0°C and the air is supersaturated with respect to

water. Similarly, cloud ice is predicted to form by sublimation of vapor when $T < 0^{\circ}\text{C}$ and the air is supersaturated with respect to ice.

Differences:

1. *Water vapor may not be a source for rain or snow by depositional growth because the excess water vapor with respect to its saturation value over water and ice is first used to form cloud liquid and ice water. This results because, in the present model flow, processes occurring under the same phase (liquid or ice) are called sequentially.*

2. *For simplicity, the prediction of cloud ice formation was parameterized in a similar manner as the prediction of cloud water, instead of using initiation and depositional growth processes, as described in Rutledge and Hobbs (1983). Also, homogeneous nucleation of cloud ice crystals at temperatures colder than -40°C is not taken into account.*

Cloud liquid as a source: Cloud liquid is a source of vapor by evaporation of cloud droplets when the air is subsaturated with respect to water. It may be a source of cloud ice by instantaneous freezing if evaporation cooling yields T to become less than 0°C , and some cloud water is still available after saturation with respect to ice is reached. Cloud water is a source of rain through two different mechanisms: (1) autoconversion of cloud droplets to form rain drops; and (2) collection of cloud droplets by rain drops falling through the free atmosphere. Finally, cloud water may also be a source of snow by riming ($T < 0^{\circ}\text{C}$) or rain ($T \geq 0^{\circ}\text{C}$) by collection of snow falling through warm layers.

3. *At present, cloud liquid droplets and cloud ice crystals do not cohabit: $T = 0^{\circ}\text{C}$ is the temperature threshold between the liquid and ice phases. The Bergeron process, or depositional growth of cloud ice at the expense of cloud water (if $-40^{\circ}\text{C} < T < 0^{\circ}\text{C}$), is not included.*

Cloud ice as a source: As for cloud liquid water, cloud ice water is a source of water vapor by evaporation of cloud ice crystals when the air is subsaturated with respect to ice. Otherwise, cloud ice is a source of snow through two different mechanisms: (1) conversion of ice crystals to form snow; and (2) collection of ice crystals by snow falling through the free atmosphere. Instantaneous melting of cloud ice to form cloud water occurs if T is equal or greater than 0°C .

4. *The accretion of cloud ice by rain to form snow (depending on the amount of rain) is not taken into account.*

Rain as a source: Rain may only be a source of water vapor by evaporation of rain drops while falling through subsaturated layers.

5. *Depositional growth of rain cannot happen in the present version of the model. The accretion of rain by cloud ice to form snow (depending on the amount of rain), and the accretion of rain by snow to produce snow (depending upon the amount of rain and snow) are not taken into account.*

Snow as a source: As for rain, snow may be a source of water vapor by evaporation while falling through subsaturated layers for which $T < 0^{\circ}\text{C}$. Also, snow may be a source of rain by melting if it falls through layers for which $T \geq 0^{\circ}$.

6. *As for rain, depositional growth of snow does not occur.*

2.2 Model flow

Assuming initial vertical profiles of temperature, water vapor, cloud water, cloud ice, rain, and snow mixing ratios, the model flow is as follows (refer to Fig3):

The water vapor, cloud water, cloud ice, rain, and snow mixing ratios, and the temperature are corrected after each microphysical process has been applied. Condensation/evaporation (PCOND) and sublimation/evaporation (PSUB) processes are called first. PCOND is applied for $T \geq 0^{\circ}\text{C}$ whereas PSUB is applied for $T < 0^{\circ}\text{C}$. The relative humidity (RH) is then less or equal to 100% across the whole atmospheric column. The subroutine PSMLTI is called next to remove any cloud ice present in layers for which $T \geq 0^{\circ}\text{C}$ ¹, or freeze any cloud water which may be present in layers for which $T < 0^{\circ}\text{C}$ ². Under supersaturation conditions, PCOND and PSUB yield an increase of the cloud liquid (ice) water mixing ratios which may become greater than their respective threshold values for rain drops and snow flakes to form. The autoconversion processes of cloud liquid droplets

¹In some cases, the sublimation of water vapor to form cloud ice may raise the temperature above the freezing level, and cloud ice must melt to form cloud water.

²This particular case occurs when evaporation of cloud water to vapor yields a cooling of the temperature below the freezing level, and some cloud water is still available after RH reaches 100 %.

to rain drops (PRAUT), and cloud ice crystals to snow (PSAUT) are applied next to remove large droplets and crystals to form rain and snow. The subroutines RWFALL and SNFALL which simulate the continuous falling of rain and snow across the atmospheric column, once rain drops and snow flakes have been predicted to form, as well as PSMLT (continuous melting of snow while snow is falling through layers for which $T \geq 0^{\circ}\text{C}$, precede the calls to any evaporation or accretion processes. The falling of rain through the atmosphere leads to an enhancement of the rain mixing ratio by accretion of the cloud water by rain drops if $\text{RH} = 100\%$ (PRACW), or to a decrease of the rain mixing ratio by evaporation if $\text{RH} < 100\%$ (PREVP). Similarly, the falling of snow through atmospheric layers for which $T < 0^{\circ}\text{C}$ yields an enhancement of the snow mixing ratio by accretion of cloud ice crystals (PSACI) and cloud liquid water droplets (PSACW) by snow flakes if $\text{RH} = 100\%$, or to a decrease of the snow mixing ratio by evaporation if $\text{RH} < 100\%$ (PSEVP).

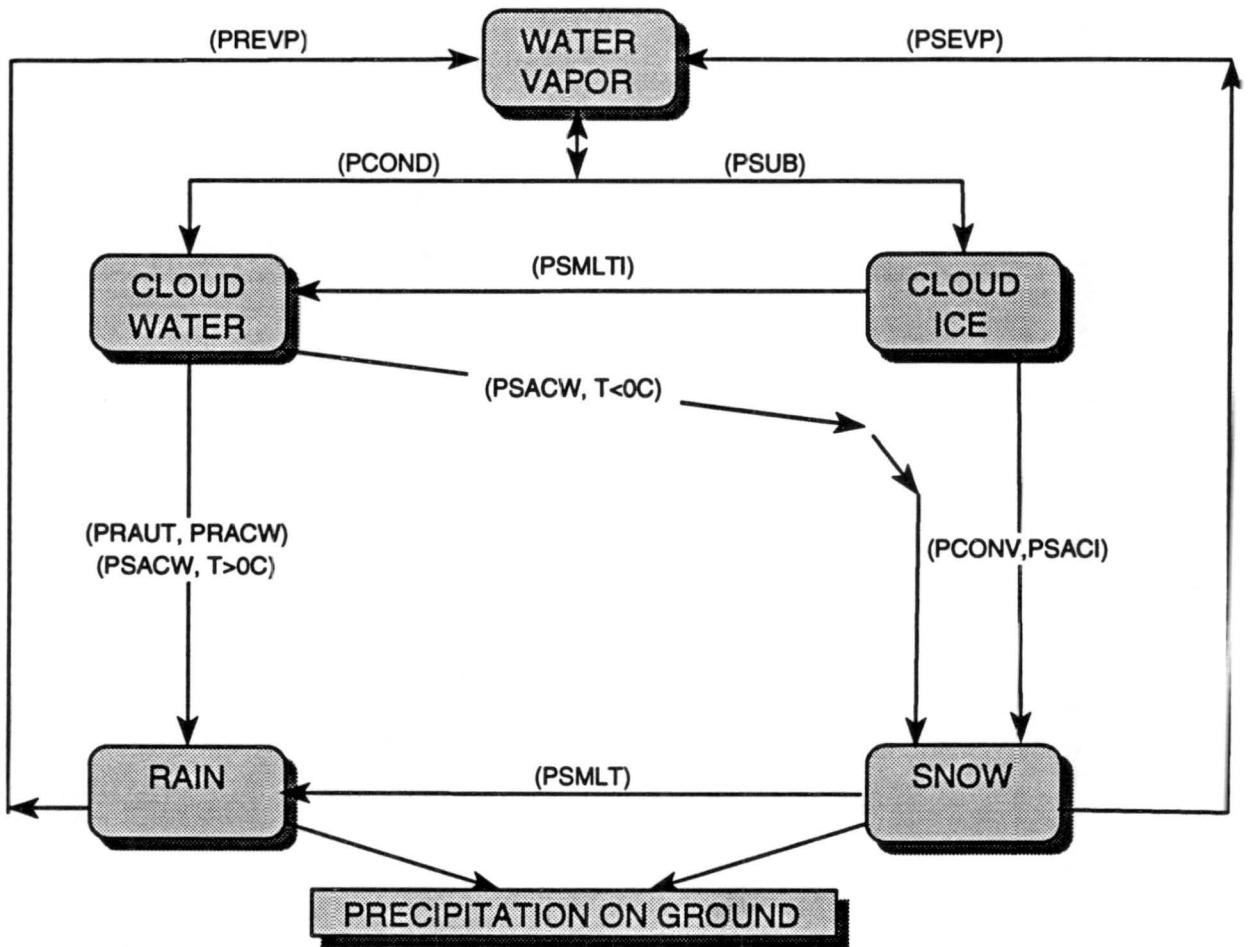
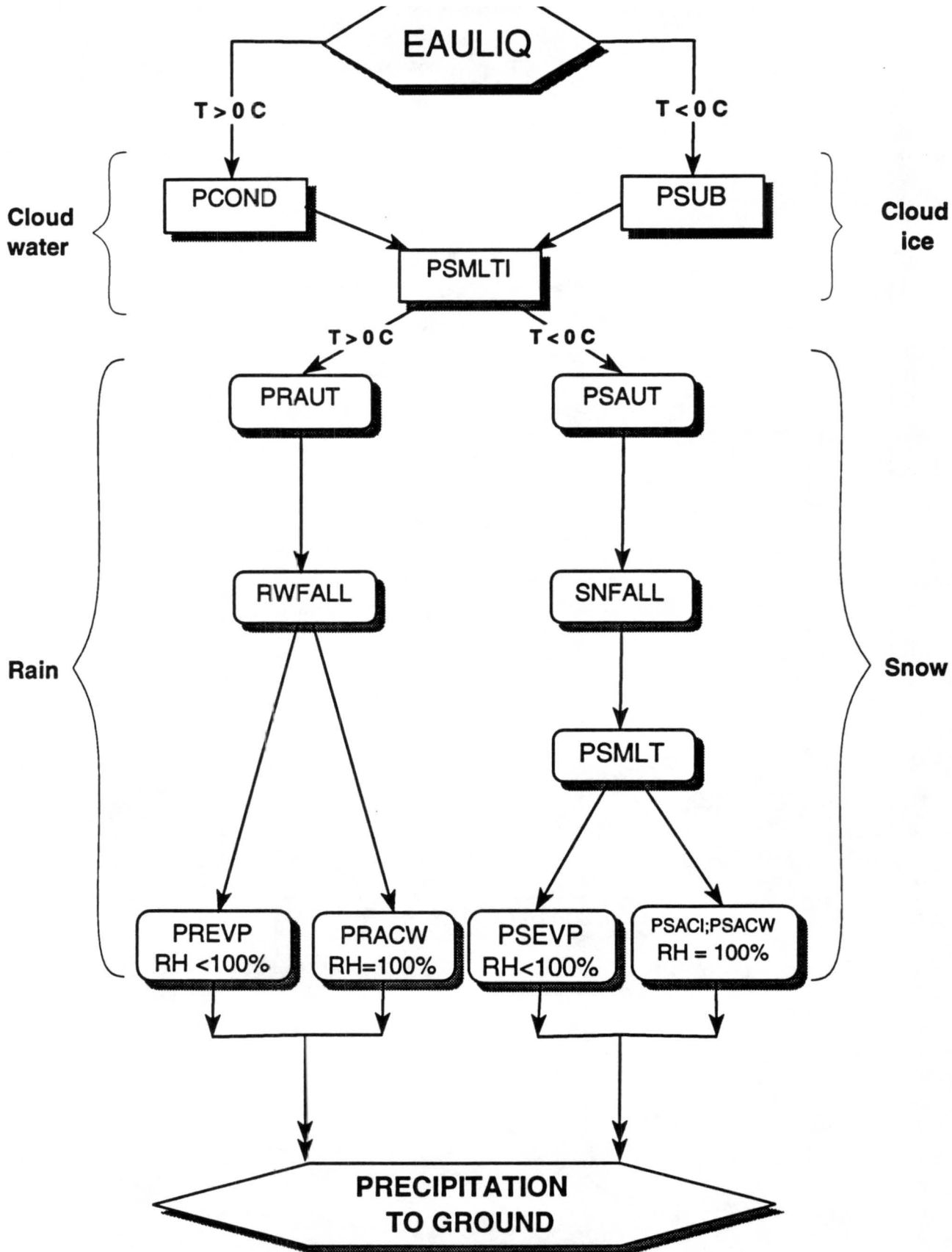


Figure 2: Schematic illustration of the cloud microphysics processes.





 : instantaneous process
 : finite rate process

Figure 3: Schematic illustration of the model flow.

3 CLOUD MICROPHYSICS

Definitions and values of variables and constants described in this section are listed in Appendix A.

3.1 Rain and snow size distributions

It is assumed that the sizes of the rain and snow particles are distributed continuously, according to an inverse exponential distribution. Rain is assumed to follow the size distribution derived by Marshall and Palmer (1948) while the size distribution of snow flakes is given by Gunn and Marshall (1958). The size distributions of rain and snow may be respectively written:

$$N_{DR} = N_{0R} \exp(-\lambda_R D_R) dD_R, \quad (1)$$

and,

$$N_{DS} = N_{0S} \exp(-\lambda_S D_S) dD_S. \quad (2)$$

The values of N_{0R} and N_{0S} given by Houze et al. (1979) are used. λ_R and λ_S are the slope factors of the size distribution for rain and snow respectively, and may be expressed as:

$$\lambda_R = \left(\frac{\pi \rho_L N_{0R}}{\rho q_r} \right)^{0.25}, \quad (3)$$

and,

$$\lambda_S = \left(\frac{\pi \rho_S N_{0S}}{\rho q_s} \right)^{0.25}. \quad (4)$$

3.2 Mass-weighted fallspeeds

Rain drops and snow flakes are assumed to fall at their mass-weighted fallspeeds.

For rain this fallspeed is defined as:

$$\bar{V}_R = \frac{\int_0^\infty N_{DR}(D_R) M(D_R) V_R(D_R) dD_R}{\int_0^\infty N_{DR}(D_R) M(D_R) dD_R}, \quad (5)$$

where $M(D_R) = \pi/6(\rho_L D_R^3)$. Following the experimental results of Gunn and Kinzer (1949), $V_R(D_R)$ may be parametrized as a function of D_R :

$$V_R(D_R) = -0.267 + 5.15 \times 10^3 D_R - 1.0225 \times 10^6 D_R^2 + 7.55 \times 10^7 D_R^3, \quad (6)$$

where the drop diameter D_R is in m. and V_R is in ms^{-1} . Using Eqs. (1), (5), and (6), \bar{V}_R may be rewritten as:

$$\bar{V}_R = (-0.267 + 206. \times 10^2 \lambda_R^{-1} - 2.045 \times 10^7 \lambda_R^{-2} + 9.06 \times 10^9 \lambda_R^{-3}) \left(\frac{p_0}{p} \right)^{0.4}, \quad (7)$$

where λ_R (m^{-1}) is given by Eq. (3).

For snow, it is assumed that snow crystals consist of aggregates of dendrites which mass-weighted fallspeed may be expressed as (Locatelli and Hobbs, 1974):

$$V_S(D_S) = a'' D_S^b \left(\frac{p_0}{p} \right)^{0.4}, \quad (8)$$

where it is assumed that $M(D_S) = \pi/6(\rho_S D_S^3)$. From Eqs. (2), (5), (8), \bar{V}_S may be rewritten as:

$$\bar{V}_S = a'' \frac{\Gamma(4+b)}{6} \lambda_S^{-b} \left(\frac{p_0}{p} \right)^{0.4}. \quad (9)$$

where λ_S (m^{-1}) is given by Eq. (4). Figure 4 shows the distribution of the mean terminal velocity for rain and snow versus the rain and snow contents.

3.3 Sources and sinks of the water continuity variables

3.3.1 Condensation of water vapor/Evaporation of cloud water (PCOND)

Condensation of water vapor to cloud water takes place when the water vapor mixing ratio exceeds its saturation value with respect to water. The excess specific humidity with respect to its saturation value over water is obtained by iterating the following equation:

$$\Delta q_c = (q_v - q_{sw}) \left[\left(1 + \frac{L_v}{c_p} \frac{dq_{sw}}{dT} \right) \right]^{-1}, \quad (10)$$

where

$$\frac{dq_{sw}}{dT} = q_{sw} \frac{p}{p - e_{sw}} \frac{d \ln e_{sw}}{dT}. \quad (11)$$

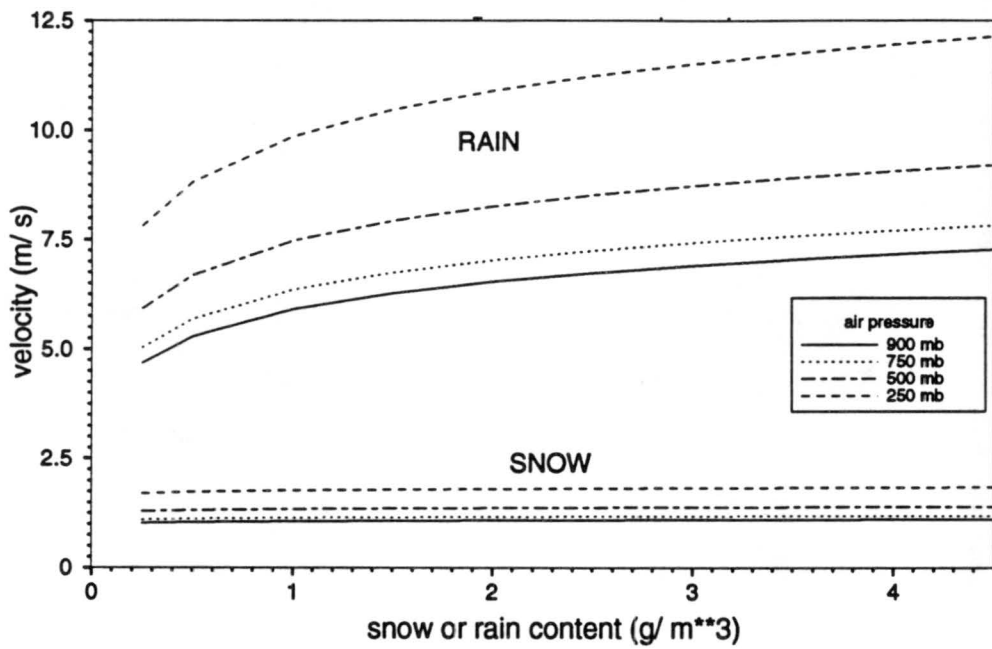


Figure 4: Mass-weighted mean terminal velocity for rain and snow at prescribed pressure levels. The four top curves are for rain. The four bottom curves are for snow.

If $q_v < q_{sw}$, the cloud water evaporates.

Condensation of water vapor/evaporation of cloud water is an instantaneous process. The condensation rate (PCOND) is dependent of the model time-step and expressed as:

$$\text{PCOND} = \frac{\Delta q_c}{\Delta t}. \quad (12)$$

3.3.2 Autoconversion of cloud water (PRAUT)

Collisions of cloud water droplets with each other lead to the continuous formation of rain drops. Following Kessler (1969), the autoconversion rate of cloud droplets to rain drops (PRAUT) may be written:

$$\text{PRAUT} = \alpha(q_c - q_{c0}), \quad (13)$$

where α is a rate coefficient and q_{c0} is a mass threshold value for autoconversion. The value of α given by Kessler (1969) is used whereas q_{c0} was deduced from airborne observations of cloud water and rain water contents in warm stratiform clouds (Rutledge and Hobbs, 1983). PRAUT is not an instantaneous process. It is shown to be highly sensitive to the threshold value q_{c0} while changes in α do not strongly modify the overall microphysics (Weinstein, 1970).

3.3.3 Collection of cloud water by rain water (PRACW)

The collection of cloud water to rain water is assumed to follow the continuous collection equation:

$$\frac{dM(D_R)}{dt} = \frac{\pi}{4} E_{RC} D_R^2 V_R(D_R) q_c. \quad (14)$$

Multiplying Eq. (14) by Eq. (1) and integrating yields:

$$\text{PRACW} = \frac{\pi}{4} E_{RC} N_{0R} q_c \left(\frac{p_0}{p}\right)^{0.4} \times \left[\frac{a_0 \Gamma(3)}{\lambda_R^3} + \frac{a_1 \Gamma(4)}{\lambda_R^4} + \frac{a_2 \Gamma(5)}{\lambda_R^5} + \frac{a_3 \Gamma(6)}{\lambda_R^6} \right], \quad (15)$$

Equation (15) may also be expressed as a function of q_r as:

$$\text{PRACW} = q_c q_r \times \frac{E_{RC}}{4} \left(\frac{\rho}{\rho_L}\right) \left(\frac{p_0}{p}\right)^{0.4} \times \left[a_0 \Gamma(3) \lambda_R + a_1 \Gamma(4) + \frac{a_2 \Gamma(5)}{\lambda_R} + \frac{a_3 \Gamma(6)}{\lambda_R^2} \right]. \quad (16)$$

3.3.4 Evaporation of rain water (PREVP)

The evaporation of rain water (PREVP) is calculated if the air is subsaturated with respect to water and the evaporation of cloud water (PCOND) is insufficient to remove the subsaturation. Similarly, if the air is supersaturated with respect to water, growth by condensation may occur. From Byers (1965), the continuous growth equation may be written as:

$$\frac{dM(D_R)}{dt} = \frac{2\pi D_R(S-1)F}{A' + B'}, \quad (17)$$

where

$$A' = \frac{L_v}{K_a T} \left(\frac{L_v M_w}{R^* T} - 1 \right), \quad (18)$$

and

$$B' = \frac{R^* T}{\chi M_w e_{sw}}. \quad (19)$$

The values of A' and B' given by Pruppacher and Klett (1978) are used. F is a ventilation factor which may be written as (Beard and Pruppacher, 1971):

$$F = 0.78 + 0.31 S_c^{1/3} R_e^{1/2}. \quad (20)$$

The total evaporation rate is then obtained by substituting Eq. (20) into Eq. (17), multiplying by Eq. (1), and integrating over all drop sizes, or:

$$\text{PREVP} = \frac{2\pi N_{0R}(S-1)}{\rho(A' + B')} \times \left[\frac{0.78}{\lambda_R^2} + 0.31 \frac{(a'\rho/\mu)^{1/2}}{\lambda_R^3} \Gamma(3) \left(\frac{p_0}{p} \right)^{0.2} \right]. \quad (21)$$

Equation (21) may also be written as a function of q_r to show the dependence between the evaporation rate and the rain water amount, or:

$$\text{PREVP} = q_r \times \frac{2(S-1)}{\rho_L(A' + B')} \times \left[0.78 \lambda_R^2 + 0.31 (a'\rho/\mu)^{1/2} \lambda_R \Gamma(3) \left(\frac{p_0}{p} \right)^{0.2} \right]. \quad (22)$$

To make the integration more manageable, it is assumed that, in Eq. (21), $V_R(D_R) = a'D_R$, which still gives good accuracy.

3.3.5 Sublimation of water vapor/Evaporation of cloud ice (PSUB)

Sublimation of water vapor to cloud ice takes place when the water vapor mixing ratio exceeds its saturation value with respect to ice. As for the condensation rate (PCOND), PSUB is an instantaneous process. The excess specific humidity with respect to its saturation value over ice is obtained by iterating the following equation:

$$\Delta q_i = (q_v - q_{si}) \left[1 + \frac{L_s}{c_p} \frac{dq_{si}}{dT} \right]^{-1}, \quad (23)$$

where

$$\frac{dq_{si}}{dT} = q_{si} \frac{p}{p - e_{si}} \frac{d \ln e_{si}}{dT}. \quad (24)$$

Similarly, if $q_v < q_{si}$, cloud ice is predicted to evaporate. The sublimation rate (PSUB) is dependent upon the model time-step and expressed as:

$$\text{PSUB} = \frac{\Delta q_i}{\Delta t}. \quad (25)$$

3.3.6 Autconversion of cloud ice to snow (PSAUT)

The conversion of cloud ice to snow (PSAUT) follows the parametrization originally proposed by Kessler (1969) to simulate the collision-coalescence process for cloud droplets. The formulation is similar to Eq. (13):

$$\text{PSAUT} = \beta(q_i - q_{i0}), \quad (26)$$

where β is a rate coefficient which is temperature dependent, and q_{i0} is a threshold amount for aggregation to occur.

The relationship used for β is:

$$\beta = 10^{-3} \exp[.025(T - T_0)], \quad (27)$$

which is a crude parametrization of the dependence of aggregation efficiency on crystal structure which, in turn, is temperature dependent.

3.3.7 Collection of cloud ice by snow (PSACI)

The collection of cloud ice by snow (PSACI) is parametrized in the same manner as the collection of cloud water by rain water (PRACW) by using the continuous collection equation:

$$\frac{dM(D_S)}{dt} = \frac{\pi}{4} E_{SI} D_S^2 V_S(D_S) q_i. \quad (28)$$

Multiplying Eq. (28) by Eq. (2), using Eq. (8), and integrating over all particle sizes yields:

$$\text{PSACI} = \frac{\pi a'' q_i E_{SI} N_{0S}}{4} \left(\frac{p_0}{p} \right)^{0.4} \frac{\Gamma(b+3)}{\lambda_S^{b+3}}, \quad (29)$$

where λ_S is given by Eq. (4).

Equation (29) may also be expressed as a function of q_s as:

$$\text{PSACI} = q_i q_s \times \frac{E_{SI}}{4} \left(\frac{\rho}{\rho_L} \right) \left(\frac{p_0}{p} \right)^{0.4} \frac{\Gamma(b+3)}{\lambda_S^{b-1}}. \quad (30)$$

3.3.8 Collection of cloud water by snow (PSACW)

For $T < 0^\circ\text{C}$, the collection of cloud water by snow (PSACW) leads to growth by riming. For $T \geq 0^\circ\text{C}$, (PSACW) represents the rate at which melting snow accretes cloud droplets, which is a source for rain. The parametrization is similar to Eq. (29):

$$\text{PSACW} = \frac{\pi a'' q_c E_{SC} N_{0S}}{4} \left(\frac{p_0}{p} \right)^{0.4} \frac{\Gamma(b+3)}{\lambda_S^{b+3}}, \quad (31)$$

where the continuous collection equation has been used. As Eq. (28), Eq. (31) may also be written as:

$$\text{PSACW} = q_c q_s \times \frac{E_{SC}}{4} \left(\frac{\rho}{\rho_L} \right) \left(\frac{p_0}{p} \right)^{0.4} \frac{\Gamma(b+3)}{\lambda_S^{b-1}}. \quad (32)$$

3.3.9 Depositional growth of snow (PSEVP)

When the air is supersaturated with respect to ice, the growth rate of snow by deposition of (PSEVP) vapor is given by:

$$\frac{dM}{dt} = \frac{C(S_i - 1)/\epsilon_0}{A'' + B''}, \quad (33)$$

where $C = 4\bar{D}_S\epsilon_0$ is the average diameter of the snow particles. In Eq. (33),

$$A'' = \frac{L_s}{K_a T} \left(\frac{L_s M_w}{R^* T} - 1 \right), \quad (34)$$

and

$$B'' = \frac{R^* T}{\chi M_w e_{si}}, \quad (35)$$

are given by Pruppacher and Klett (1978). Multiplying Eq. (33) by Eq. (2), and integrating over all sizes of snow particles, we obtain:

$$\text{PSEVP} = \frac{4(S_i - 1)N_{0S}}{\rho(A'' + B'')} \times \left[\frac{0.65}{\lambda_S^2} + 0.44 \left(\frac{a''\rho}{\mu} \right)^{1/2} \left(\frac{p_0}{p} \right)^{0.2} \frac{\Gamma(\frac{b}{2} + \frac{5}{2})}{\lambda_S^{b/2+5/2}} \right]. \quad (36)$$

3.3.10 Melting of snow (PSMLT)

All snow upon melting is assumed to contribute to rain. The snow melted per unit time (PSMLT) is given by Mason (1971):

$$\frac{dM_{\text{melt}}}{dt} = \frac{-2\pi}{L_f \rho} K_a D_S (T - T_0) F', \quad (37)$$

where F' is a ventilation factor which is given by Thorpe and Mason (1966):

$$F' = 0.65 + 0.44 S_c^{1/3} R_e^{1/2}, \quad (38)$$

where R_e is now $V_S(D_S)D_S\rho/\mu$. Substituting Eq. (38) into Eq. (37), multiplying by Eq. (2) and integrating over all snow sizes we obtain for the melting rate of snow:

$$\text{PSMLT} = \frac{-2\pi N_{0S}}{L_f \rho} K_a (T - T_0) \left[\frac{0.65}{\lambda_S^2} + 0.44 \left(\frac{a''\rho}{\mu} \right)^{1/2} \left(\frac{p_0}{p} \right)^{0.2} \frac{\Gamma(\frac{b}{2} + \frac{5}{2})}{\lambda_S^{b/2+5/2}} \right]. \quad (39)$$

Equation (39) may also be written as a function of q_s , or:

$$\text{PSMLT} = -q_s \times \frac{2K_a(T - T_0)}{\rho_S L_f \rho} \left[0.65 \lambda_S^2 + 0.44 \left(\frac{a''\rho}{\mu} \right)^{1/2} \left(\frac{p_0}{p} \right)^{0.2} \frac{\Gamma(\frac{b}{2} + \frac{5}{2})}{\lambda_S^{b/2-3/2}} \right]. \quad (40)$$

3.3.11 Melting of cloud ice (PSMLTI)

Melted cloud ice is a source for cloud water. This process is assumed to occur instantaneously and is given by:

$$\text{PSMLTI} = q_i / \Delta t, \quad (41)$$

for $T \geq 0^\circ\text{C}$ only.

3.4 Source terms for the water continuity variables

The source terms for the five continuity variables are:

For water vapor q_v :

$$\frac{dq_v}{dt} = -[\text{PCOND} + \text{PSUB} + \text{PREVP} + \text{PSEVP}]. \quad (42)$$

For cloud water q_c :

$$\frac{dq_c}{dt} = \text{PCOND} + \text{PSMLTI} (T \geq 0^\circ\text{C}) - \text{PRAUT} - \text{PRACW} - \text{PSACW}. \quad (43)$$

For cloud ice q_i :

$$\frac{dq_i}{dt} = \text{PSUB} - \text{PSMLTI} (T \geq 0^\circ\text{C}) - \text{PSAUT} - \text{PSACI}. \quad (44)$$

For rain q_r :

$$\frac{dq_r}{dt} = \text{PREVP} + \text{PRAUT} + \text{PRACW} - \text{PSMLT} (T \geq 0^\circ\text{C}) + \text{PSACW} (T \geq 0^\circ\text{C}). \quad (45)$$

For snow q_s :

$$\frac{dq_s}{dt} = \text{PSEVP} + \text{PSACI} + \text{PSMLT} (T \geq 0^\circ\text{C}) + \text{PSACW} (T < 0^\circ\text{C}) + \text{PSAUT}. \quad (46)$$

Similarly, the source term for T is:

$$\begin{aligned} \frac{dT}{dt} = & \frac{L_v}{c_p} (\text{PCOND} + \text{PREVP}) \\ & + \frac{L_s}{c_p} (\text{PSUB} + \text{PSEVP}) \\ & + \frac{L_f}{c_p} [\text{PSMLT} - \text{PSMLTI} + \text{PSACW} (T < 0^\circ\text{C})]. \end{aligned} \quad (47)$$

3.5 Conservation of the generalized moist static energy

Using Eqs. (42), (43), (44), (45), and (46), it is obvious that under the three-phase processes, the total cloud water budget is conserved, or:

$$\frac{d}{dt}(q_v + q_c + q_r + q_i + q_s) = 0. \quad (48)$$

The conservation equation of the generalized moist static energy may be derived as follows:

Multiplying Eq. (42) by L_v and Eq. (48) by c_p , and adding them together yields:

$$\begin{aligned} \frac{d}{dt}(c_p T + L_v q_v) = & L_f (\text{PSUB} + \text{PSEVP} + \text{PSMLT} (T \geq 0^\circ\text{C}) \\ & - \text{PSMLTI} (T \geq 0^\circ\text{C}) + \text{PSACW} (T < 0^\circ\text{C})), \end{aligned} \quad (49)$$

using the relation:

$$L_s = L_c + L_f. \quad (50)$$

Multiplying Eqs. (44) and (46) by L_f , and adding them together yields:

$$\begin{aligned} \frac{d}{dt}(L_f(q_i + q_s)) = & L_f (\text{PSUB} + \text{PSEVP} + \text{PSMLT} (T \geq 0^\circ\text{C}) \\ & - \text{PSMLTI} (T \geq 0^\circ\text{C}) + \text{PSACW} (T < 0^\circ\text{C})). \end{aligned} \quad (51)$$

Finally, subtracting Eqs. (49) to (51) leads to the equation of conservation of the generalized moist static energy under the three-phase processes:

$$\frac{d}{dt}(c_p T + L_c q_v) - L_f(q_i + q_s) = 0. \quad (52)$$

In Eq. (52), it is assumed that there is no variation in the potential energy.

4 TEST OF EACH PROCESS

This section summarizes "tests" of each microphysical process listed in Table 2. The initial atmospheric profile of pressure, temperature, and water vapor mixing ratio is the standard tropical atmosphere. Results are given for a pressure level, as specified in each table caption. The model time-step is 60s. The list of symbols used in this section is given in A.

4.1 Process PCOND

4.1.1 Condensation of water vapor

Initial conditions: The subroutine PCOND is run alone. Initially, the water vapor mixing ratio is less than its saturation value with respect to water. The advection of water vapor to start supersaturation conditions is prescribed and equal to $1. \times 10^{-2} \text{kg kg}^{-1} \text{day}^{-1}$.

Table 3: **pcond:** p=958.5mb - t=60s

Initial conditions		Final conditions	
T_0	297.0000	T	297.0023
q_{wv0}	$.19797950 \times 10^{-1}$	qwv	$.19797030 \times 10^{-1}$
q_{satw0}	$.19794250 \times 10^{-1}$	qsatw	$.19797021 \times 10^{-1}$
q_{cw0}	.0	qcw	$.92551681 \times 10^{-6}$
q_{rw0}	.0	qrw	.0
q_{ci0}	.0	qci	.0
q_{ri0}	.0	qri	.0

Change in T, qwv, qcw, qrw, qci, qri:

$$\begin{aligned}
 dT &= +.38371352 \times 10^{-4} \text{ K s}^{-1} \\
 dq_{wv} &= -.15425280 \times 10^{-7} \text{ kg kg}^{-1} \text{ s}^{-1} \\
 dq_{cw} &= +.15425280 \times 10^{-7} \text{ kg kg}^{-1} \text{ s}^{-1} \\
 dq_{rw} &= .0 \\
 \text{div}(q_{rw}) &= .0 \\
 dq_{ci} &= .0 \\
 dq_{ri} &= .0 \\
 \text{div}(q_{ri}) &= .0
 \end{aligned}$$

Therefore,

$$dq_{wv} + dq_{cw} + dq_{rw} - \text{div}(q_{rw}) + dq_{ci} + dq_{ri} - \text{div}(q_{ri}) = 0.$$

Conservation of energy:

$$\begin{aligned}
 C_p dT &= +.03856321 \text{ J kg}^{-1} \text{ s}^{-1} \\
 L_c dq_{wv} &= -.03856320 \text{ J kg}^{-1} \text{ s}^{-1} \\
 L_f (dq_{ci} + dq_{ri} - \text{div}(q_{ri})) &= .0
 \end{aligned}$$

Therefore,

$$\begin{aligned}\Delta E &= C_p dT + L_c dq_{wv} - L_f (dq_{ci} + dq_{ri} - \text{div}(q_{ri})) \\ &= .79472867 \times 10^{-8} \text{ J kg}^{-1} \text{ s}^{-1} \\ \frac{\Delta E}{C_p dT} &= .20608470 \times 10^{-6}\end{aligned}$$

4.1.2 Evaporation of cloud water

Initial conditions: The initial profile of the water vapor mixing ratio is one close to supersaturation conditions with respect to water. A constant vertical profile of $q_{cw} = 1. \times 10^{-3} \text{ kg kg}^{-1}$ in layers for which $T \geq 0^\circ \text{ C}$ is assigned.

Table 4: pcond: p=958.5mb - t=60s

Initial conditions		Final conditions	
T_0	297.0000	T	296.9957
q_{wv0}	$.19787304 \times 10^{-1}$	q_{wv}	$.19789004 \times 10^{-1}$
q_{satw_0}	$.19794250 \times 10^{-1}$	q_{satw}	$.19789000 \times 10^{-1}$
q_{cw_0}	$.1 \times 10^{-2}$	q_{cw}	$.99830330 \times 10^{-3}$
q_{rw_0}	.0	q_{rw}	.0
q_{ci_0}	.0	q_{ci}	.0
q_{ri_0}	.0	q_{ri}	.0

Change in T, q_{wv} , q_{cw} , q_{rw} , q_{ci} , q_{ri} :

$$\begin{aligned}dT &= -.70344280 \times 10^{-4} \text{ K s}^{-1} \\ dq_{wv} &= +.28278400 \times 10^{-7} \text{ kg kg}^{-1} \text{ s}^{-1} \\ dq_{cw} &= -.28278400 \times 10^{-7} \text{ kg kg}^{-1} \text{ s}^{-1} \\ dq_{rw} &= .0 \\ \text{div}(q_{rw}) &= .0 \\ dq_{ci} &= .0 \\ dq_{ri} &= .0 \\ \text{div}(q_{ri}) &= .0\end{aligned}$$

Therefore,

$$dq_{wv} + dq_{cw} + dq_{rw} - \text{div}(q_{rw}) + dq_{ci} + dq_{ri} - \text{div}(q_{ri}) = 0.$$

Conservation of energy:

$$\begin{aligned}C_p dT &= -.07069600 \text{ J kg}^{-1} \text{ day}^{-1} \\ L_c dq_{wv} &= +.07069599 \text{ J kg}^{-1} \text{ day}^{-1} \\ L_f (dq_{ci} + dq_{ri} - \text{div}(q_{ri})) &= .0\end{aligned}$$

Therefore,

$$\begin{aligned}\Delta E &= -.79472867 \times 10^{-8} \text{ J kg}^{-1} \text{ s}^{-1} \\ \frac{\Delta E}{C_p dT} &= .11241493 \times 10^{-6}\end{aligned}$$

Remarks: It may occur that evaporation cooling yields T to drop below the freezing level and that some cloud water may remain. In that case, cloud water is instantaneously frozen as cloud ice in the subroutine PSM_{TI}.

4.2 Process PRAUT

Initial conditions: The subroutine PCOND is called prior to PRAUT to remove supersaturation conditions and form cloud water. The increase of the cloud water mixing ratios with time yields the autoconversion process to start.

Figure 5 illustrates the increase of (a) the cloud water, and (b) rain mixing ratios, and (c) the temperature in layers for which $T \geq 0^\circ\text{C}$.

Table 5: **pra**ut: p=958.5mb - t=60s

Initial conditions		Final conditions	
T_0	300.1695	T	300.1732
q_{wv0}	$.24061630 \times 10^{-1}$	q_{wv}	$.24060143 \times 10^{-1}$
q_{satw_0}	$.24054690 \times 10^{-1}$	q_{satw}	$.24060150 \times 10^{-1}$
q_{cw_0}	$.11782124 \times 10^{-2}$	q_{cw}	$.11792121 \times 10^{-2}$
q_{rw_0}	$.96055533 \times 10^{-4}$	q_{rw}	$.96535222 \times 10^{-4}$
q_{ci_0}	.0	q_{ci}	.0
q_{ri_0}	.0	q_{ri}	.0

Change in T, q_{wv} , q_{cw} , q_{rw} , q_{ci} , q_{ri} :

$$\begin{aligned}
 dT &= +.61333220 \times 10^{-4} \text{ K s}^{-1} \\
 dq_{wv} &= -.24655951 \times 10^{-7} \text{ kg kg}^{-1} \text{ s}^{-1} \\
 dq_{cw} &= +.16661086 \times 10^{-7} \text{ kg kg}^{-1} \text{ s}^{-1} \\
 dq_{rw} &= +.79948652 \times 10^{-8} \text{ kg kg}^{-1} \text{ s}^{-1} \\
 \text{div}(q_{rw}) &= .0 \\
 dq_{ci} &= .0 \\
 dq_{ri} &= .0 \\
 \text{div}(q_{ri}) &= .0
 \end{aligned}$$

Therefore,

$$dq_{wv} + dq_{cw} + dq_{rw} - \text{div}(q_{rw}) + dq_{ci} + dq_{ri} - \text{div}(q_{ri}) = 0.$$

Conservation of energy:

$$\begin{aligned}
 C_p dT &= +.06163988 \text{ J kg}^{-1} \text{ s}^{-1} \\
 L_c dq_{wv} &= -.06163988 \text{ J kg}^{-1} \text{ s}^{-1} \\
 L_f (dq_{ci} + dq_{ri} - \text{div}(q_{ri})) &= .0
 \end{aligned}$$

Therefore,

$$\begin{aligned}\Delta E &= .0 \text{ J kg}^{-1} \text{ s}^{-1} \\ \frac{\Delta E}{C_p dT} &= .0\end{aligned}$$

4.3 Process RWFALL

Initial conditions: Constant vertical profile of $qrw = 1. \times 10^{-3} \text{ kg kg}^{-1}$ in layers for which $T \geq 0^\circ\text{C}$.

Only the subroutine RWFALL is run and the rain falls freely through the atmosphere.

Figure 6 shows the falling of rain through layers for which $T \geq 0^\circ\text{C}$.

Table 6: **rwfall:** t=60s

pressure (mb)	Initial conditions	Final conditions
596.0	$qrw_0 \ .10000000 \times 10^{-2}$	$qrw \ .76161600 \times 10^{-3}$
760.0	$qrw_0 \ .10000000 \times 10^{-2}$	$qrw \ .98548050 \times 10^{-3}$
958.5	$qrw_0 \ .10000000 \times 10^{-2}$	$qrw \ .98679530 \times 10^{-3}$

$$p = 596.0\text{mb} : \text{div}(qrw) = -.39730680 \times 10^{-5} \text{ kg kg}^{-1} \text{ s}^{-1}$$

$$p = 760.0\text{mb} : \text{div}(qrw) = -.24199280 \times 10^{-6} \text{ kg kg}^{-1} \text{ s}^{-1}$$

$$p = 958.5\text{mb} : \text{div}(qrw) = -.22008021 \times 10^{-6} \text{ kg kg}^{-1} \text{ s}^{-1}$$

4.4 Process PRACW

Initial conditions: Constant vertical profiles of $qcw = 1. \times 10^{-3}$ and $qrw = 1. \times 10^{-3}$ are prescribed in layers for which $T \geq 0^\circ\text{C}$. Figure 7 shows (a) the decrease of the cloud water mixing ratio with time, and (b) the corresponding increase of the rain mixing ratio.

Table 7: **pracw:** p=958.5 mb - t=60 s

Initial conditions		Final conditions	
T_0	297.00000	T	297.0000
q_{wv0}	$.14249553 \times 10^{-1}$	q_{wv}	$.14249553 \times 10^{-1}$
q_{satw_0}	$.19794250 \times 10^{-1}$	q_{satw}	$.19794250 \times 10^{-1}$
q_{cw_0}	$.10000000 \times 10^{-2}$	q_{cw}	$.81742410 \times 10^{-3}$
q_{rw_0}	$.10000000 \times 10^{-2}$	q_{rw}	$.11825760 \times 10^{-2}$
q_{ci_0}	.0	q_{ci}	.0
q_{ri_0}	.0	q_{ri}	.0

Change in T, qwv, qcw, qrw, qci, qri:

$$\begin{aligned}
 dT &= .0 \\
 dqwv &= .0 \\
 dqcw^3 &= -.3042933 \times 10^{-5} \text{ kg kg}^{-1} \text{ s}^{-1} \\
 dqrw &= +.3042933 \times 10^{-5} \text{ kg kg}^{-1} \text{ s}^{-1} \\
 \text{div}(qrw) &= .0 \\
 dqci &= .0 \\
 dqri &= .0 \\
 \text{div}(qri) &= .0
 \end{aligned}$$

Therefore,

$$dqwv + dqcw + dqrw - \text{div}(qrw) + dqci + dqri - \text{div}(qri) = .0$$

Conservation of energy:

$$\begin{aligned}
 C_p dT &= .0 \text{ J kg}^{-1} \text{ s}^{-1} \\
 L_c dqwv &= .0 \text{ J kg}^{-1} \text{ s}^{-1} \\
 L_f (dqci + dqri - \text{div}(qri)) &= .0 \text{ J kg}^{-1} \text{ s}^{-1}
 \end{aligned}$$

Therefore,

$$\begin{aligned}
 \Delta E &= .0 \text{ J kg}^{-1} \text{ s}^{-1} \\
 \frac{\Delta E}{C_p dT} &= .0
 \end{aligned}$$

4.5 Process PREVP

Initial conditions: A constant vertical profile of $qrw = 1. \times 10^{-3} \text{ kg kg}^{-1}$ is prescribed in layers for which $T \geq 0^\circ\text{C}$. Initially, the water vapor mixing ratio is less than its saturation value with respect to water across the whole atmospheric column. Only the subroutine PREVP is run. Figure 8 shows (a) the increase of the relative humidity, (b) the decrease of the rain mixing ratio, and (c) the corresponding decrease of the air temperature.

Table 8: **prevp**: p=958.5mb - t=60s.

Initial conditions		Final conditions	
T_0	297.0000	T	296.7752
qwv_0	$.14249553 \times 10^{-1}$	qwv	$.14339912 \times 10^{-1}$
$qsatw_0$	$.19794250 \times 10^{-1}$	qsatw	$.19280493 \times 10^{-1}$
qcw_0	.0	qcw	.0
qrw_0	$.10000000 \times 10^{-2}$	qrw	$.90964170 \times 10^{-3}$
qci_0	.0	qci	.0
qri_0	.0	qri	.0

Change in T, qwv, qcw, qrw, qci, qri:

$$\begin{aligned}
 dT &= -.37462010 \times 10^{-2} \text{ K s}^{-1} \\
 dqwv &= +.15059730 \times 10^{-5} \text{ kg kg}^{-1} \text{ s}^{-1} \\
 dqcw &= .0 \\
 dqrw &= -.15059730 \times 10^{-5} \text{ kg kg}^{-1} \text{ s}^{-1} \\
 \text{div}(qrw) &= .0 \\
 dqci &= .0 \\
 dqri &= .0 \\
 \text{div}(qri) &= .0
 \end{aligned}$$

Therefore,

$$dqwv + dqcw + dqrw - \text{div}(qrw) + dqci + dqri - \text{div}(qri) = .0$$

Conservation of energy:

$$\begin{aligned}
 C_p dT &= -3.76493167 \text{ J kg}^{-1} \text{ s}^{-1} \\
 L_c dqwv &= +3.76493167 \text{ J kg}^{-1} \text{ s}^{-1} \\
 L_f (dqci + dqri - \text{div}(qri)) &= .0
 \end{aligned}$$

Therefore,

$$\begin{aligned}
 \Delta E &= .0 \text{ J kg}^{-1} \text{ s}^{-1} \\
 \frac{\Delta E}{C_p dT} &= .0
 \end{aligned}$$

4.6 Process PSUB

4.6.1 Sublimation of water vapor

Initial conditions: The subroutine PSUB is run alone. Initially, qwv is less than its saturation value with respect to ice. As in the process PCOND, the advection rate of water vapor to force supersaturation conditions to start is equal to $1. \times 10^{-2} \text{ kg kg}^{-1} \text{ day}^{-1}$.

Table 9: psub: p=230mb - t=60s

Initial conditions		Final conditions	
T_0	227.0000	T	227.0061
qwv_0	$.17198710 \times 10^{-3}$	qwv	$.16980440 \times 10^{-3}$
$qsati_0$	$.16967963 \times 10^{-3}$	qsati	$.16980440 \times 10^{-3}$
qcw_0	.0	qcw	.0
qrw_0	.0	qrw	.0
qci_0	.0	qci	$.21826940 \times 10^{-5}$
qri_0	.0	qri	.0

Change in T, qwv, qcw, qrw, qci, qri:

$$\begin{aligned}
 dT &= +.10256851 \times 10^{-3} \text{ K s}^{-1} \\
 dqwv &= -.36378240 \times 10^{-7} \text{ kg kg}^{-1} \text{ s}^{-1}
 \end{aligned}$$

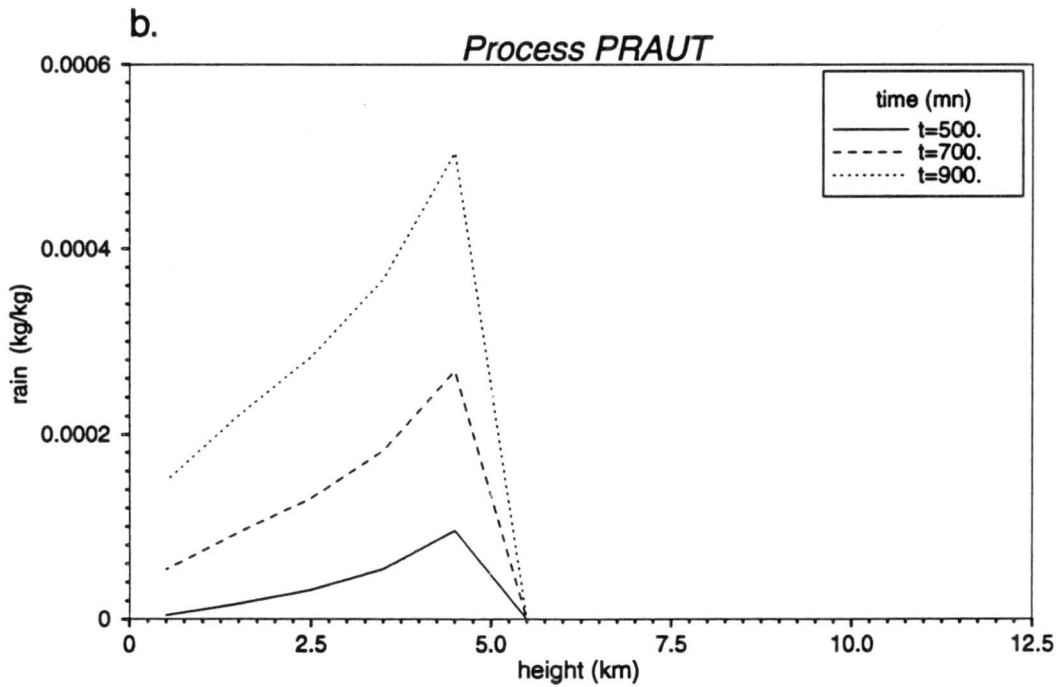
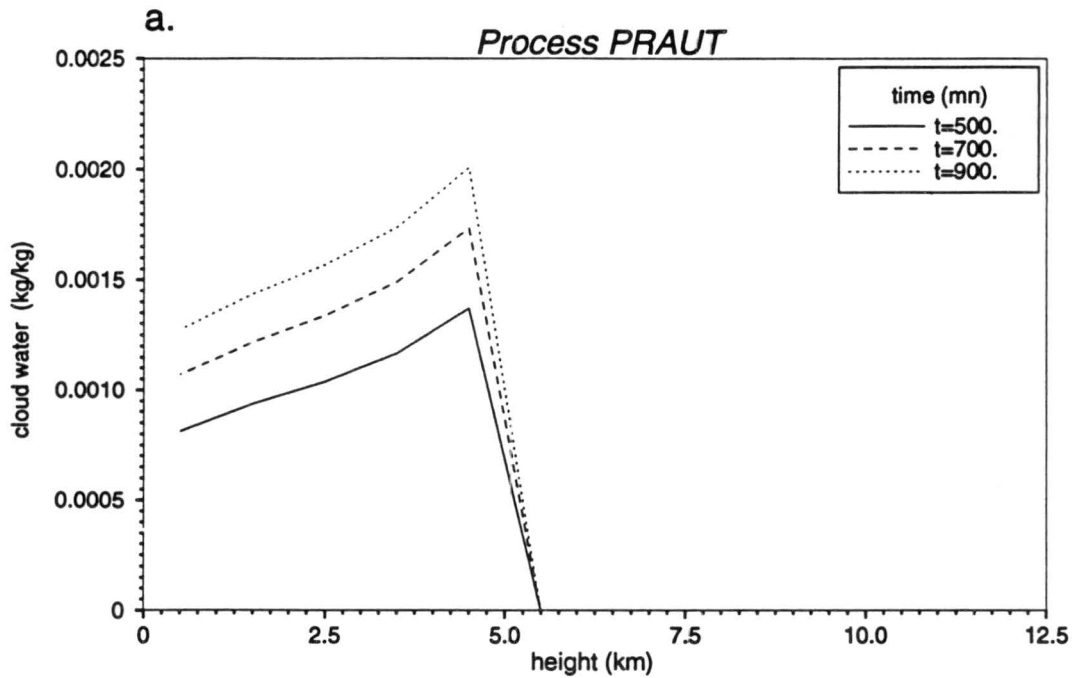


Figure 5: Process PRAUT- Increase of (a) the cloud water mixing ratio, (b) the rain mixing ratio and (c) the temperature when supersaturation occurs and rain starts to form by auto-conversion of cloud water droplets.

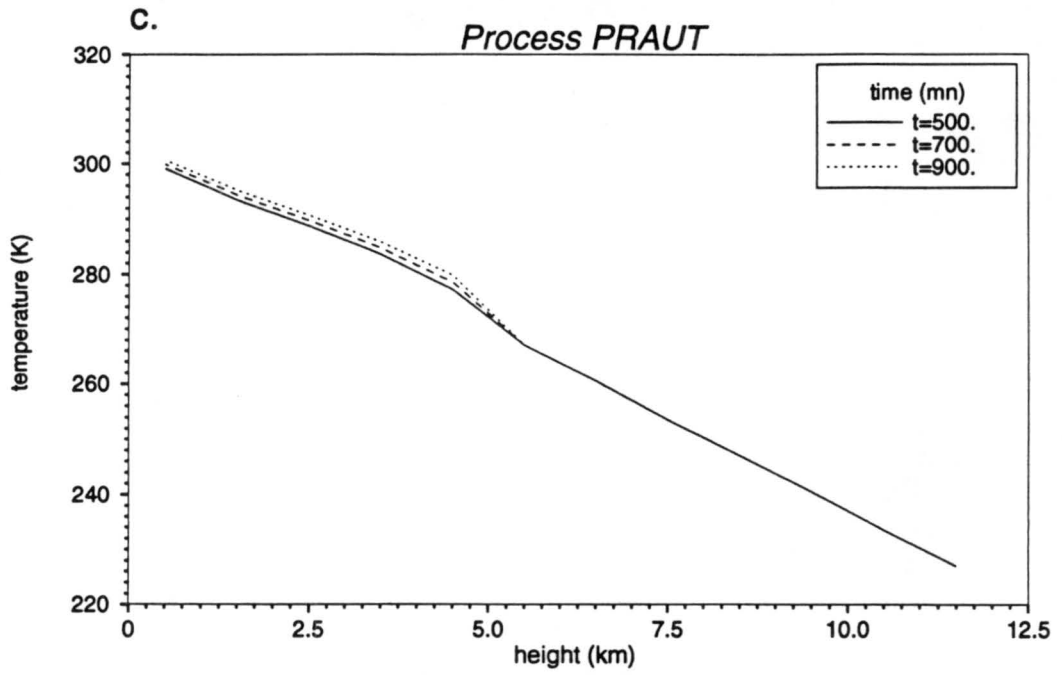


Figure 5: Process PRAUT-continued

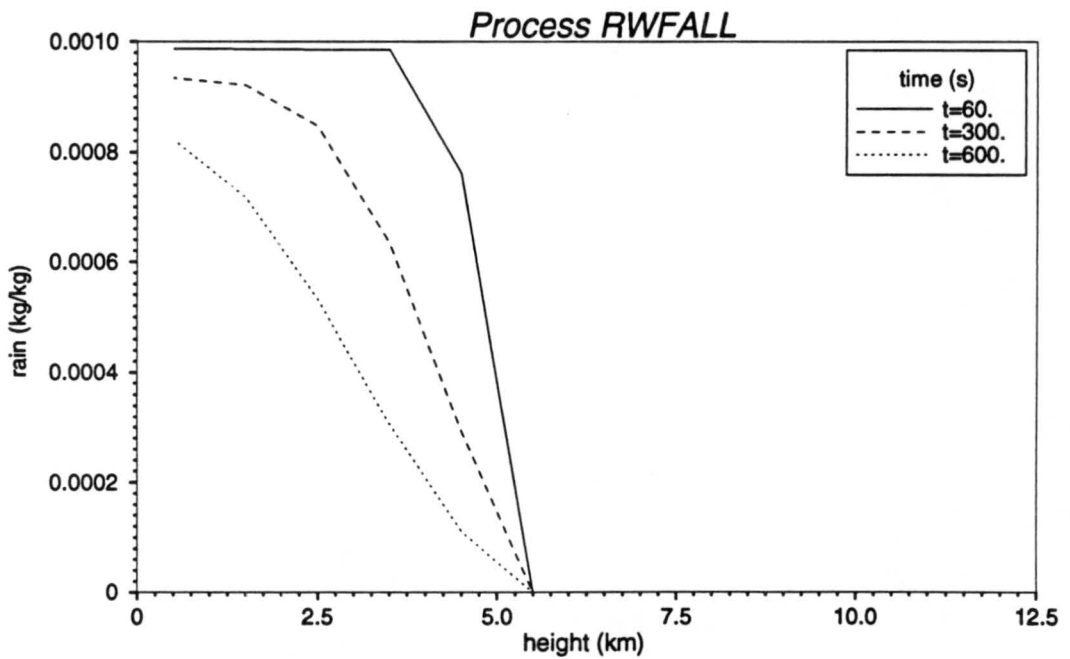


Figure 6: Process RWFALL- Falling of rain.

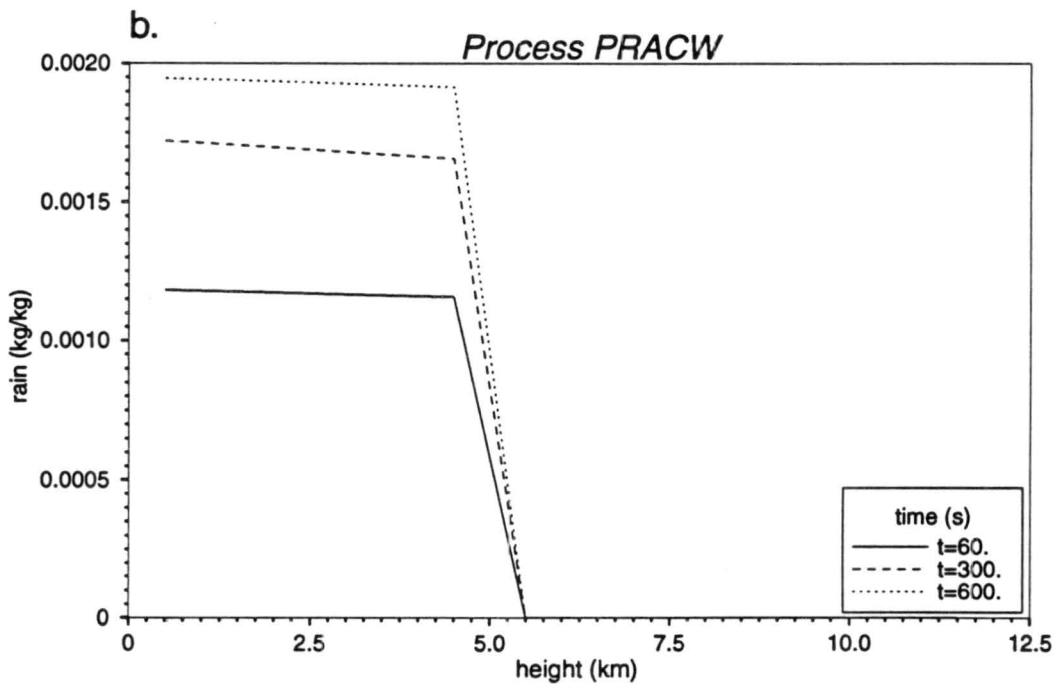
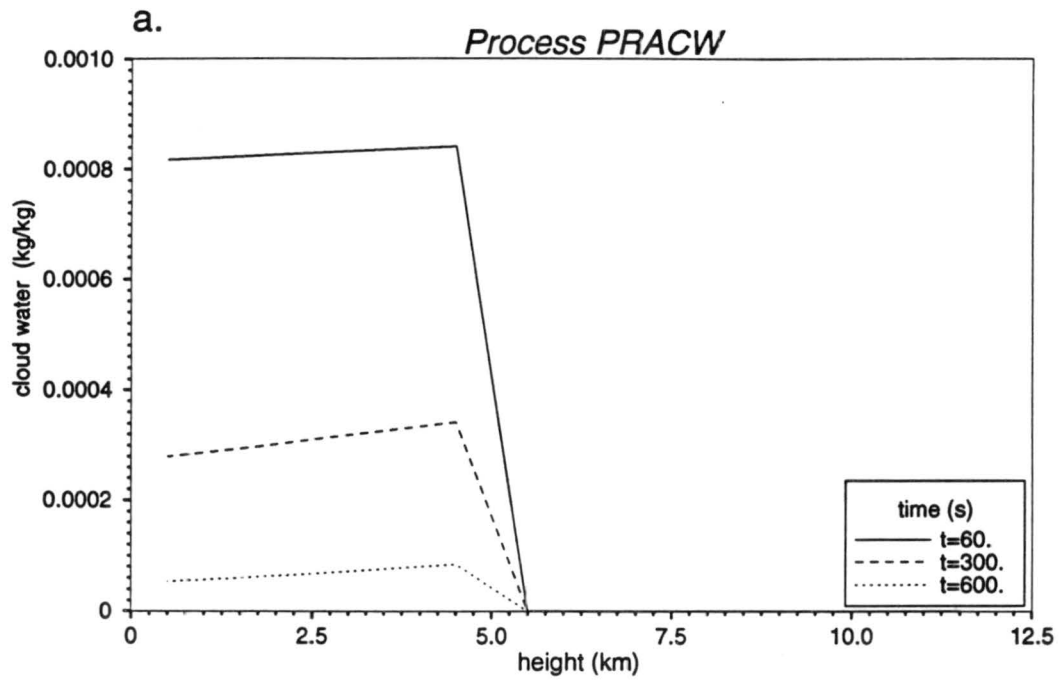


Figure 7: Process PRACW- (a) Decrease of the cloud water mixing ratio by accretion of rain, and (b) corresponding increase of the rain mixing ratio in layers for which ($T \geq 0^\circ\text{C}$).

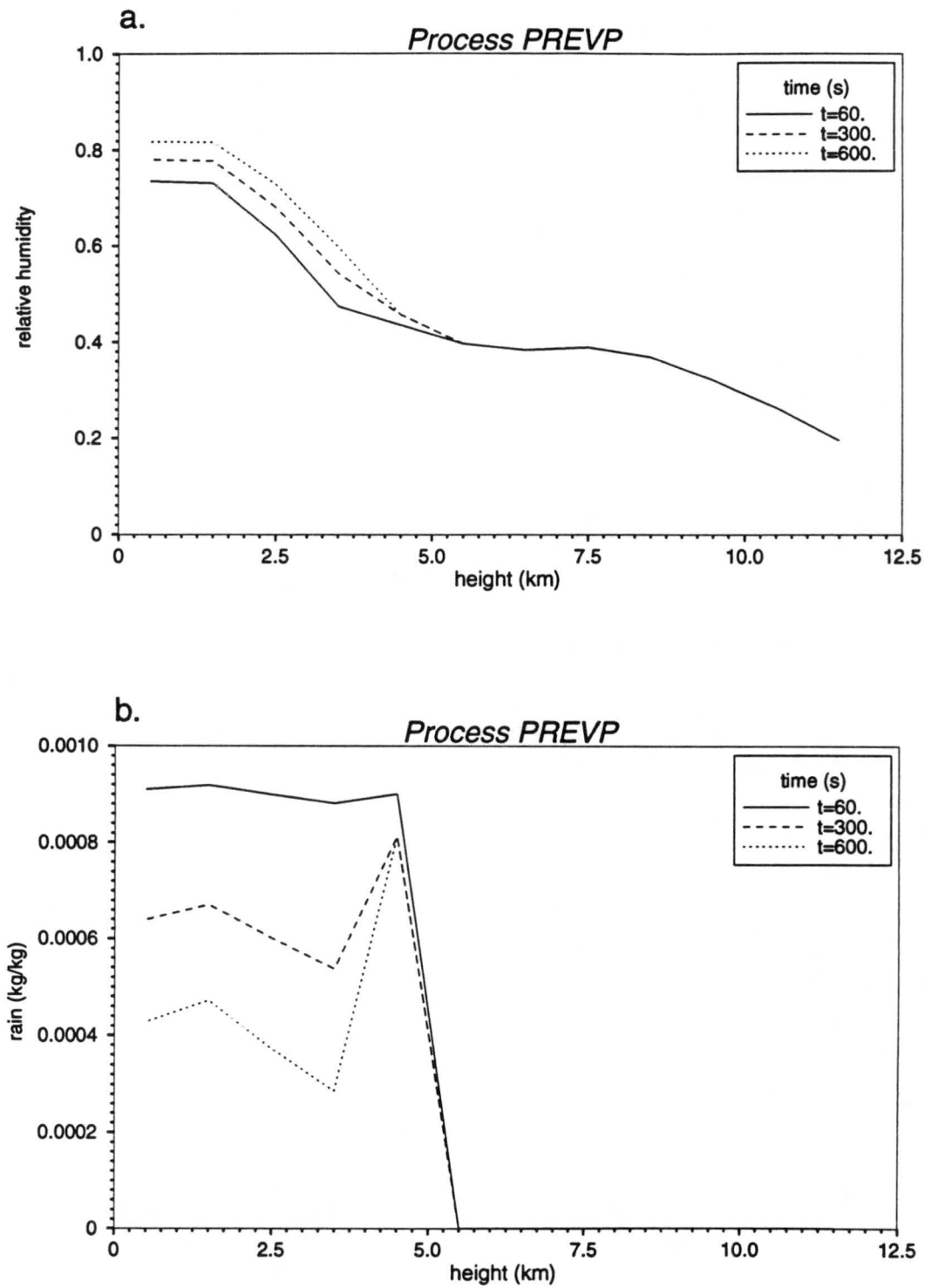


Figure 8: Process PREVP- (a) Increase of the relative humidity, (b) decrease of the rain mixing ratio, and (c) decrease of the air temperature due to evaporation cooling.

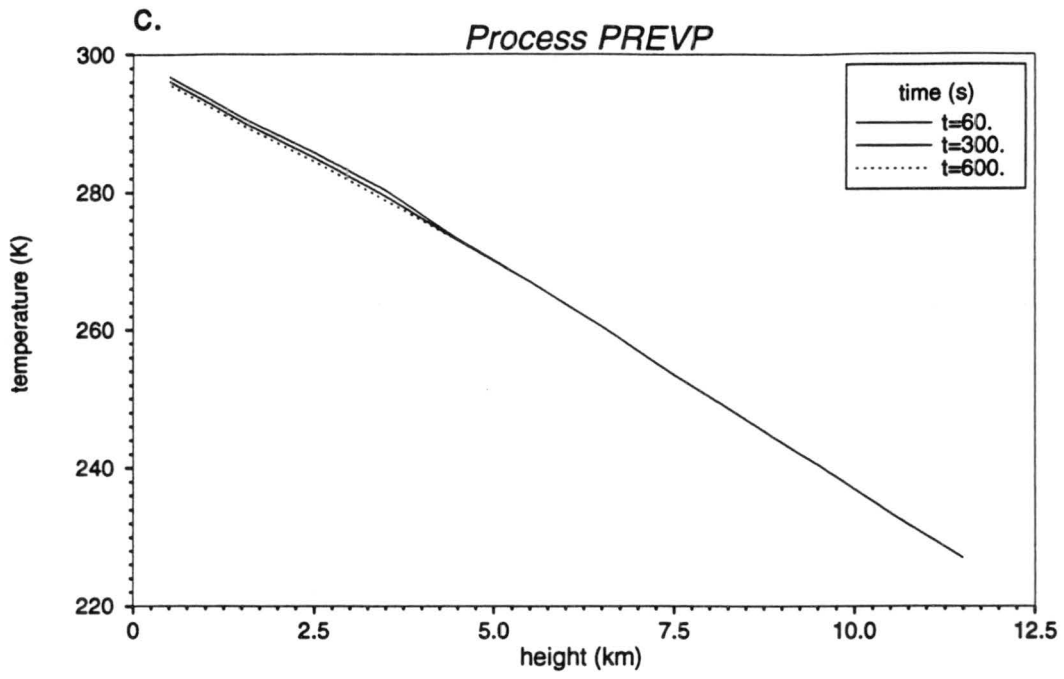


Figure 8: Process PREVP-continued

$$\begin{aligned}
dq_{cw} &= .0 \\
dq_{rw} &= .0 \\
\text{div}(q_{rw}) &= .0 \\
dq_{ci} &= +.36378240 \times 10^{-7} \text{ kg kg}^{-1} \text{ s}^{-1} \\
dq_{ri} &= .0 \\
\text{div}(q_{ri}) &= .0
\end{aligned}$$

Therefore,

$$dq_{wv} + dq_{cw} + dq_{rw} - \text{div}(q_{rw}) + dq_{ci} + dq_{ri} - \text{div}(q_{ri}) = .0$$

Conservation of energy:

$$\begin{aligned}
C_p dT &= +.10308137 \text{ J kg}^{-1} \text{ s}^{-1} \\
L_c dq_{wv} &= -.09094559 \text{ J kg}^{-1} \text{ s}^{-1} \\
L_f (dq_{ci} + dq_{ri} - \text{div}(q_{ri})) &= +.01213579 \text{ J kg}^{-1} \text{ s}^{-1}
\end{aligned}$$

Therefore,

$$\begin{aligned}
\Delta E &= -.29802322 \times 10^{-8} \text{ J kg}^{-1} \text{ s}^{-1} \\
\frac{\Delta E}{C_p dT} &= -.28911460 \times 10^{-7}
\end{aligned}$$

4.6.2 Evaporation of cloud ice

Initial conditions: The initial profile of q_{rw} is close to supersaturation conditions with respect to ice. A constant vertical profile of $q_{ci} = 1. \times 10^{-3} \text{ kg kg}^{-1}$ for layers for which $T < 0^\circ\text{C}$ is prescribed.

Table 10: **psub:** p=230mb - t=60s

Initial conditions		Final conditions	
T_0	227.0000	T	226.9815
q_{wv_0}	$.16273520 \times 10^{-3}$	q_{wv}	$.16930440 \times 10^{-3}$
q_{sati_0}	$.16967963 \times 10^{-3}$	q_{sati}	$.16930440 \times 10^{-3}$
q_{cw_0}	.0	q_{cw}	.0
q_{rw_0}	.0	q_{rw}	.0
q_{ci_0}	$.10000000 \times 10^{-2}$	q_{ci}	$.99343084 \times 10^{-3}$
q_{ri_0}	.0	q_{ri}	.0

Change in T, q_{wv} , q_{cw} , q_{rw} , q_{ci} , q_{ri} :

$$\begin{aligned}
dT &= -.30869711 \times 10^{-3} \text{ K s}^{-1} \\
dq_{wv} &= +.10948640 \times 10^{-6} \text{ kg kg}^{-1} \text{ s}^{-1} \\
dq_{cw} &= .0 \\
dq_{rw} &= .0 \\
\text{div}(q_{rw}) &= .0 \\
dq_{ci} &= -.10948640 \times 10^{-6} \text{ kg kg}^{-1} \text{ s}^{-1} \\
dq_{ri} &= .0 \\
\text{div}(q_{ri}) &= .0
\end{aligned}$$

Therefore,

$$dqwv + dqcw + dqrw - \text{div}(qrw) + dqci + dqri - \text{div}(qri) = .0$$

Conservation of energy:

$$\begin{aligned} C_p dT &= -.31024067 \text{ J kg}^{-1} \text{ s}^{-1} \\ L_c dqwv &= +.19403827 \text{ J kg}^{-1} \text{ s}^{-1} \\ L_f (dqci + dqri - \text{div}(qri)) &= -.03652466 \text{ J kg}^{-1} \text{ s}^{-1} \end{aligned}$$

Therefore,

$$\begin{aligned} \Delta E &= -.11920929 \times 10^{-7} \text{ J kg}^{-1} \text{ s}^{-1} \\ \frac{\Delta E}{C_p dT} &= -.38424790 \times 10^{-7} \end{aligned}$$

4.7 Process PSAUT

Initial conditions: The subroutine PSUB is called prior to PSAUT to remove supersaturation conditions and form cloud ice. The increase of the cloud ice mixing ratios with time yields the autoconversion process to start.

Figure 9 illustrates the increase of (a) the cloud ice, and (b) rain mixing ratios, and (c) the temperature in layers for which $T < 0^\circ\text{C}$ due to latent heat release.

Table 11: **psaut**: p=230mb - t=60s

Initial conditions		Final conditions	
T_0	240.5215	T	240.5374
qwv_0	$.78646873 \times 10^{-3}$	qwv	$.78084302 \times 10^{-3}$
$qsati_0$	$.77952430 \times 10^{-3}$	qsati	$.78084302 \times 10^{-3}$
qcw ₀	.0	qcw	.0
qrw ₀	.0	qrw	.0
qci ₀	$.43408572 \times 10^{-2}$	qci	$.43450021 \times 10^{-2}$
qri ₀	$.45438910 \times 10^{-3}$	qri	$.45586991 \times 10^{-3}$

Change in T, qwv, qcw, qrw, qci, qri:

$$\begin{aligned} dT &= +.26436120 \times 10^{-3} \text{ K s}^{-1} \\ dqwv &= -.93761657 \times 10^{-7} \text{ kg kg}^{-1} \text{ s}^{-1} \\ dqcw &= .0 \\ dqrw &= .0 \\ \text{div}(qrw) &= .0 \\ dqci &= +.69081337 \times 10^{-7} \text{ kg kg}^{-1} \text{ s}^{-1} \\ dqri &= +.24680318 \times 10^{-7} \text{ kg kg}^{-1} \text{ s}^{-1} \\ \text{div}(qri) &= .0 \end{aligned}$$

Therefore,

$$dqwv + dqcw + dqrw - \text{div}(qrw) + dqci + dqri - \text{div}(qri) = -.16666667 \times 10^{-9} \text{ kg kg}^{-1} \text{ s}^{-1}$$

Conservation of energy:

$$\begin{aligned}C_p dT &= .26568302 \text{ J kg}^{-1} \text{ s}^{-1} \\L_c dq_{wv} &= .23440417 \text{ J kg}^{-1} \text{ s}^{-1} \\L_f(dq_{ci} + dq_{ri} - \text{div}(q_{ri})) &= .03127889 \text{ J kg}^{-1} \text{ s}^{-1}\end{aligned}$$

Therefore,

$$\begin{aligned}\Delta E &= .79472867 \times 10^{-8} \text{ J kg}^{-1} \text{ s}^{-1} \\ \frac{\Delta E}{C_p dT} &= -.29912660 \times 10^{-7}\end{aligned}$$

4.8 Process SNFALL

Initial conditions: Constant vertical profile of $q_{ri} = 1. \times 10^{-3} \text{ kg kg}^{-1}$ in layers for which $T < 0^\circ\text{C}$.

Only the subroutine SNFALL is run and the snow falls freely through the atmosphere.

Figure 10 shows the falling of rain with time. The top layer ($p = 230\text{mb}$) is rapidly depleted of snow and snow starts to fall through layers initially without snow ($T \geq 0^\circ\text{C}$), as for the layer $p = 596\text{mb}$. Below the top layer, as for the layer $p = 405\text{mb}$, the change in the snow content remains small because the loss of snow at the base of each layer is compensated by snow falling from the layer above.

Table 12: snfall: t=60s

pressure (mb)	Initial conditions	Final conditions
230.	$q_{ri_0} \ .10000000 \times 10^{-2}$	$q_{ri} \ .96066691 \times 10^{-3}$
405.	$q_{ri_0} \ .10000000 \times 10^{-2}$	$q_{ri} \ .99828910 \times 10^{-3}$
596.	$q_{ri_0} \ .10000000 \times 10^{-2}$	$q_{ri} \ .25587500 \times 10^{-4}$

$$p = 230\text{mb} : \text{div}(q_{ri}) = -.65555200 \times 10^{-6} \text{ kg kg}^{-1} \text{ s}^{-1}$$

$$p = 405\text{mb} : \text{div}(q_{ri}) = -.28516790 \times 10^{-7} \text{ kg kg}^{-1} \text{ s}^{-1}$$

$$p = 596\text{mb} : \text{div}(q_{ri}) = -.42645830 \times 10^{-6} \text{ kg kg}^{-1} \text{ s}^{-1}$$

4.9 Process PSACI

Initial conditions: Constant vertical profiles of $q_{ci} = 1. \times 10^{-3} \text{ kg kg}^{-1}$ and $q_{ri} = 1. \times 10^{-3} \text{ kg kg}^{-1}$ are prescribed in layers for $T < 0^\circ\text{C}$. Only the subroutine PSACI is run. Figure 11 shows (a) the decrease of the cloud ice mixing ratio due to the collection by snow and (b) the corresponding increase of the snow mixing ratio.

Table 13: **psaci**: p=230mb - t=60s

Initial conditions		Final conditions	
T_0	227.0000	T	227.0000
qwv_0	$.33098152 \times 10^{-4}$	qwv	$.33098152 \times 10^{-4}$
$qsati_0$	$.16967963 \times 10^{-3}$	$qsati$	$.16967963 \times 10^{-3}$
qcw_0	.0	qcw	.0
qrw_0	.0	qrw	.0
qci_0	$.10000000 \times 10^{-2}$	qci	$.98542263 \times 10^{-3}$
qri_0	$.10000000 \times 10^{-2}$	qri	$.10145774 \times 10^{-2}$

Change in T, qwv, qcw, qrw, qci, qri:

$$\begin{aligned}
 dT &= .0 \\
 dqwv &= .0 \\
 dqcw &= .0 \\
 dqrw &= .0 \\
 \text{div}(qrw) &= .0 \\
 dqci &= -.24295670 \times 10^{-6} \text{ kg kg}^{-1} \text{ s}^{-1} \\
 dqri &= +.24295670 \times 10^{-6} \text{ kg kg}^{-1} \text{ s}^{-1} \\
 \text{div}(qri) &= .0
 \end{aligned}$$

Therefore,

$$dqwv + dqcw + dqrw - \text{div}(qrw) + dqci + dqri - \text{div}(qri) = .0$$

Conservation of energy:

$$\begin{aligned}
 C_p dT &= .0 \text{ J kg}^{-1} \text{ s}^{-1} \\
 L_c dqwv &= .0 \text{ J kg}^{-1} \text{ s}^{-1} \\
 L_f(dqci + dqri - \text{div}(qri)) &= .0 \text{ J kg}^{-1} \text{ s}^{-1}
 \end{aligned}$$

Therefore,

$$\begin{aligned}
 \Delta E &= 0. \text{ J kg}^{-1} \text{ s}^{-1} \\
 \frac{\Delta E}{C_p dT} &= 0.
 \end{aligned}$$

4.10 Process PSACW

Initial conditions: Constant vertical profiles of $q_{cw} = 1. \times 10^{-3} \text{kg kg}^{-1}$ and $q_{ri} = 1. \times 10^{-3} \text{kg kg}^{-1}$ are prescribed across the whole atmosphere to simulate the accretion of cloud water by snow if $T < 0^{\circ}\text{C}$ or the accretion of cloud water by melting snow if $T \geq 0^{\circ}\text{C}$.

4.10.1 Accretion of cloud water by snow

Table 14: psacw: p=525.5mb - t=60s

Initial conditions		Final conditions	
T_0	267.0000	T	267.0501
q_{wv_0}	$.17240843 \times 10^{-2}$	q_{wv}	$.17240843 \times 10^{-2}$
q_{sati_0}	$.43348232 \times 10^{-2}$	q_{sati}	$.43537444 \times 10^{-2}$
q_{cw_0}	$.10000000 \times 10^{-2}$	q_{cw}	$.84891080 \times 10^{-3}$
q_{rw_0}	.0	q_{rw}	.0
q_{ci_0}	.0	q_{ci}	.0
q_{ri_0}	$.10000000 \times 10^{-2}$	q_{ri}	$.11510893 \times 10^{-2}$

Change in T, q_{wv} , q_{cw} , q_{rw} , q_{ci} , q_{ri} :

$$\begin{aligned}
 dT &= +.83587714 \times 10^{-3} \text{ K s}^{-1} \\
 dq_{wv} &= .0 \\
 dq_{cw} &= -.25181550 \times 10^{-5} \text{ kg kg}^{-1} \text{ s}^{-1} \\
 dq_{rw} &= .0 \\
 \text{div}(q_{rw}) &= .0 \\
 dq_{ci} &= .0 \\
 dq_{ri} &= +.25181550 \times 10^{-5} \text{ kg kg}^{-1} \text{ s}^{-1}
 \end{aligned}$$

Therefore,

$$dq_{wv} + dq_{cw} + dq_{rw} - \text{div}(q_{rw}) + dq_{ci} + dq_{ri} - \text{div}(q_{ri}) = .0$$

Conservation of energy:

$$\begin{aligned}
 C_p dT &= .799888033 \text{ J kg}^{-1} \text{ s}^{-1} \\
 L_c dq_{wv} &= .0 \\
 L_f (dq_{ci} + dq_{ri} - \text{div}(q_{ri})) &= .799888033 \text{ J kg}^{-1} \text{ s}^{-1}
 \end{aligned}$$

Therefore,

$$\begin{aligned}
 \Delta E &= 0. \text{ J kg}^{-1} \text{ s}^{-1} \\
 \frac{\Delta E}{C_p dT} &= 0. \text{ J kg}^{-1} \text{ s}^{-1}
 \end{aligned}$$

4.10.2 Accretion of cloud water by melting snow

Note: In Table 15, q_{ri} is the mixing ratio for melting snow.

Table 15: psacw: p=596mb - t=60s

Initial conditions		Final conditions	
T_0	273.5000	T	273.5000
qwv_0	$.27353931 \times 10^{-2}$	qwv	$.27353931 \times 10^{-2}$
$qsatw_0$	$.66075972 \times 10^{-2}$	$qsati$	$.66075972 \times 10^{-2}$
qcw_0	$.10000000 \times 10^{-2}$	qcw	$.84523903 \times 10^{-3}$
qrw_0	.0	qrw	$.15476101 \times 10^{-3}$
qci_0	.0	qci	.0
qri_0	$.10000000 \times 10^{-2}$	qri	$.00000000 \times 10^{-2}$

Change in T, qwv, qcw, qrw, qci, qri:

$$\begin{aligned}
dT &= .0 \\
dqwv &= .0 \\
dqcw &= -.25181550 \times 10^{-5} \text{ kg kg}^{-1} \text{ s}^{-1} \\
dqrw &= +.25181550 \times 10^{-5} \text{ kg kg}^{-1} \text{ s}^{-1} \\
\text{div}(qrw) &= .0 \\
dqci &= .0 \\
dqri &= .0 \\
\text{div}(qri) &= .0
\end{aligned}$$

Therefore,

$$dqwv + dqcw + dqrw - \text{div}(qrw) + dqci + dqri - \text{div}(qri) = .0$$

Conservation of energy:

$$\begin{aligned}
C_p dT &= .0 \text{ J kg}^{-1} \text{ s}^{-1} \\
L_c dqwv &= .0 \text{ J kg}^{-1} \text{ s}^{-1} \\
L_f(dqci + dqri - \text{div}(qri)) &= .0 \text{ J kg}^{-1} \text{ s}^{-1}
\end{aligned}$$

Therefore,

$$\begin{aligned}
C_p dT + L_c dqwv - \\
L_f(dqci + dqri - \text{div}(qri)) &= .0 \text{ J kg}^{-1} \text{ s}^{-1} \\
\Delta(\text{energ}) &= .0 \text{ J kg}^{-1} \text{ s}^{-1}
\end{aligned}$$

4.11 Process PSEVP

Initial conditions: Constant vertical profile $qri = 1. \times 10^{-3} \text{ kg kg}^{-1}$ for layers with $T < 0^\circ\text{C}$. Initially, the water vapor mixing ratio is less than its saturation value with respect to ice across the whole atmospheric column. Only the subroutine PSEVP is run.

Figure 12 shows (a) the increase of the relative humidity, (b) the decrease of the snow mixing ratio, and (c) the decrease of the air temperature due to evaporation cooling.

Table 16: psevp: p=230mb - t=60s

Initial conditions		Final conditions	
T_0	227.0000	T	226.9754
q_{wv0}	$.33098152 \times 10^{-4}$	q _{wv}	$.41817664 \times 10^{-4}$
q_{sati0}	$.16967963 \times 10^{-3}$	q _{sati}	$.16872110 \times 10^{-3}$
q_{cw0}	.0	q _{cw}	.0
q_{rw0}	.0	q _{rw}	.0
q_{ci0}	.0	q _{ci}	.0
q_{ri0}	$.10000000 \times 10^{-2}$	q _{ri}	$.99128053 \times 10^{-3}$

Change in T, q_{wv}, q_{cw}, q_{rw}, q_{ci}, q_{ri}:

$$\begin{aligned}
 dT &= -.40974480 \times 10^{-3} \text{ K s}^{-1} \\
 dq_{wv} &= +.14532521 \times 10^{-6} \text{ kg kg}^{-1} \text{ s}^{-1} \\
 dq_{cw} &= .0 \\
 dq_{rw} &= .0 \\
 \text{div}(q_{rw}) &= .0 \\
 dq_{ci} &= .0 \\
 dq_{ri} &= -.14532521 \times 10^{-6} \text{ kg kg}^{-1} \text{ s}^{-1} \\
 \text{div}(q_{ri}) &= .0
 \end{aligned}$$

Therefore,

$$dq_{wv} + dq_{cw} + dq_{rw} - \text{div}(q_{rw}) + dq_{ci} + dq_{ri} - \text{div}(q_{ri}) = .0$$

Conservation of energy:

$$\begin{aligned}
 C_p dT &= -.41179352 \text{ J kg}^{-1} \text{ s}^{-1} \\
 L_c dq_{wv} &= +.36331303 \text{ J kg}^{-1} \text{ s}^{-1} \\
 L_f (dq_{ci} + dq_{ri} - \text{div}(q_{ri})) &= -.04848049 \text{ J kg}^{-1} \text{ s}^{-1}
 \end{aligned}$$

Therefore,

$$\begin{aligned}
 \Delta E &= -.11920929 \times 10^{-7} \text{ J kg}^{-1} \text{ s}^{-1} \\
 \frac{\Delta E}{C_p dT} &= .28948802 \times 10^{-7}
 \end{aligned}$$

At the end of ten minutes, the relative humidity in that layer has increased from 19.5% to 55.7%.

4.12 Process PSMLT

Initial conditions: Constant vertical distribution of $q_{ri} = 1.-3 \text{ kg kg}^{-1}$ for layers with $T < 0^\circ\text{C}$, plus the first layer which T is above the freezing level. The subroutine PSMLT is run alone.

Figure 13 illustrates the decrease of the snow mixing ratio at the expense of (b) the rain mixing ratio.

Table 17: psm1t: p=596mb - t=60s

Initial conditions		Final conditions	
T_0	273.5000	T	273.4893
q_{wv_0}	$.27353931 \times 10^{-2}$	q_{wv}	$.27353931 \times 10^{-2}$
q_{satw_0}	$.66075970 \times 10^{-2}$	q_{satw}	$.66024030 \times 10^{-2}$
q_{cw_0}	.0	q_{cw}	.0
q_{rw_0}	.0	q_{rw}	$.32317071 \times 10^{-4}$
q_{ci_0}	.0	q_{ci}	.0
q_{ri_0}	$.10000000 \times 10^{-2}$	q_{ri}	$.96768300 \times 10^{-3}$

Change in T, q_{wv} , q_{cw} , q_{rw} , q_{ci} , q_{ri} :

$$\begin{aligned}
 dT &= -.17878900 \times 10^{-3} \text{ K s}^{-1} \\
 dq_{wv} &= .0 \\
 dq_{cw} &= .0 \\
 dq_{rw} &= +.53861790 \times 10^{-6} \text{ kg kg}^{-1} \text{ s}^{-1} \\
 \text{div}(q_{rw}) &= .0 \\
 dq_{ci} &= .0 \\
 dq_{ri} &= -.53861790 \times 10^{-6} \text{ kg kg}^{-1} \text{ s}^{-1} \\
 \text{div}(q_{ri}) &= .0
 \end{aligned}$$

Therefore,

$$dq_{wv} + dq_{cw} + dq_{rw} - \text{div}(q_{rw}) + dq_{ci} + dq_{ri} - \text{div}(q_{ri}) = 0.$$

Conservation of energy:

$$\begin{aligned}
 C_p dT &= -.17968300 \text{ J kg}^{-1} \text{ s}^{-1} \\
 L_c dq_{wv} &= .0 \\
 L_f (dq_{ci} + dq_{ri} - \text{div}(q_{ri})) &= -.17968300 \text{ J kg}^{-1} \text{ s}^{-1}
 \end{aligned}$$

Therefore,

$$\begin{aligned}
 \Delta E &= .0 \text{ J kg}^{-1} \text{ s}^{-1} \\
 \frac{\Delta E}{C_p dT} &= .0
 \end{aligned}$$

4.13 Process PSMLTI

Initial conditions: q_{ci} is equal to $1. \times 10^{-3} \text{ kg kg}^{-1}$ in one layer for which $T \geq 0^\circ\text{C}$. The melting is instantaneous.

Table 18: psmlti: p=596mb - t=60s

Initial conditions		Final conditions	
T_0	273.5	T	273.1681
q_{wv0}	$.27353931 \times 10^{-2}$	q_{wv}	$.27353931 \times 10^{-2}$
q_{satw_0}	$.66075972 \times 10^{-2}$	q_{satw}	$.64487910 \times 10^{-2}$
q_{cw_0}	.0	q_{cw}	$.10000000 \times 10^{-2}$
q_{rw_0}	.0	q_{rw}	.0
q_{ci_0}	$.10000000 \times 10^{-2}$	q_{ci}	.0
q_{ri_0}	.0	q_{ri}	.0

Change in T, q_{wv}, q_{cw}, q_{rw}, q_{ci}, q_{ri}:

$$\begin{aligned}
 dT &= -.55323383 \times 10^{-2} \text{ K s}^{-1} \\
 dq_{cw} &= .0 \\
 dq_{cw} &= +.16666667 \times 10^{-4} \text{ kg kg}^{-1} \text{ s}^{-1} \\
 dq_{rw} &= .0 \\
 \text{div}(q_{rw}) &= .0 \\
 dq_{ci} &= -.16666667 \times 10^{-4} \text{ kg kg}^{-1} \text{ s}^{-1} \\
 dq_{ri} &= .0 \\
 \text{div}(q_{ri}) &= .0
 \end{aligned}$$

Therefore,

$$dq_{wv} + dq_{cw} + dq_{rw} - \text{div}(q_{rw}) + dq_{ci} + dq_{ri} - \text{div}(q_{ri}) = 0.$$

Conservation of energy:

$$\begin{aligned}
 C_p dT &= -5.56 \text{ J kg}^{-1} \text{ s}^{-1} \\
 L_c dq_{wv} &= .0 \text{ J kg}^{-1} \\
 L_f (dq_{ci} + dq_{ri} - \text{div}(q_{ri})) &= -5.56 \text{ J kg}^{-1} \text{ s}^{-1}
 \end{aligned}$$

Therefore,

$$\begin{aligned}
 \Delta E &= .0 \text{ J kg}^{-1} \text{ s}^{-1} \\
 \frac{\Delta E}{C_p dT} &= .0
 \end{aligned}$$

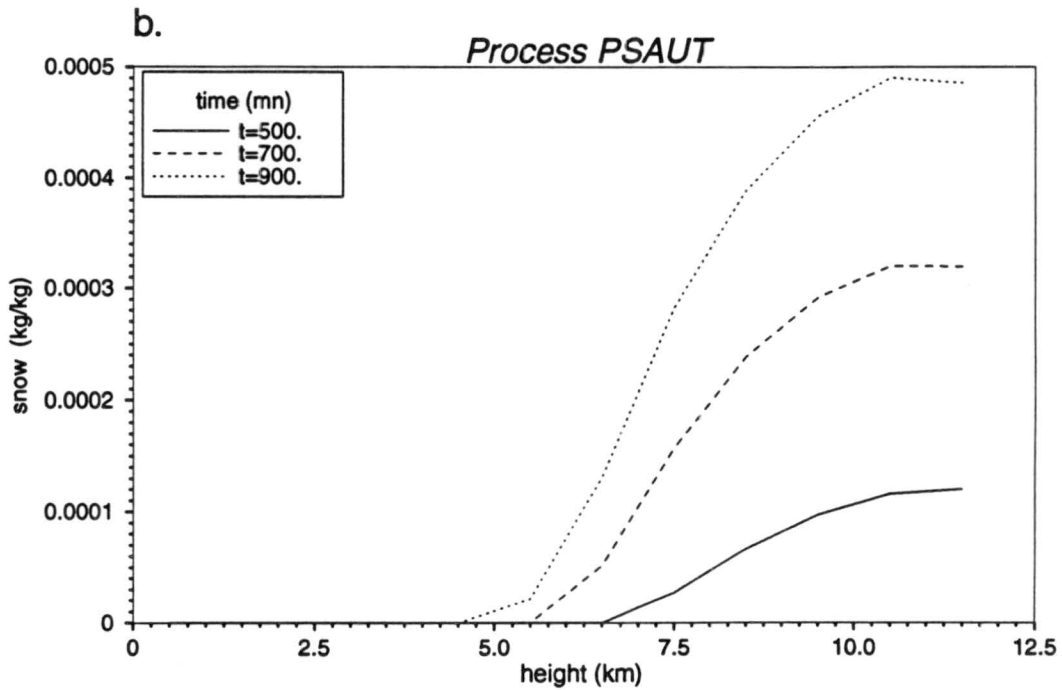
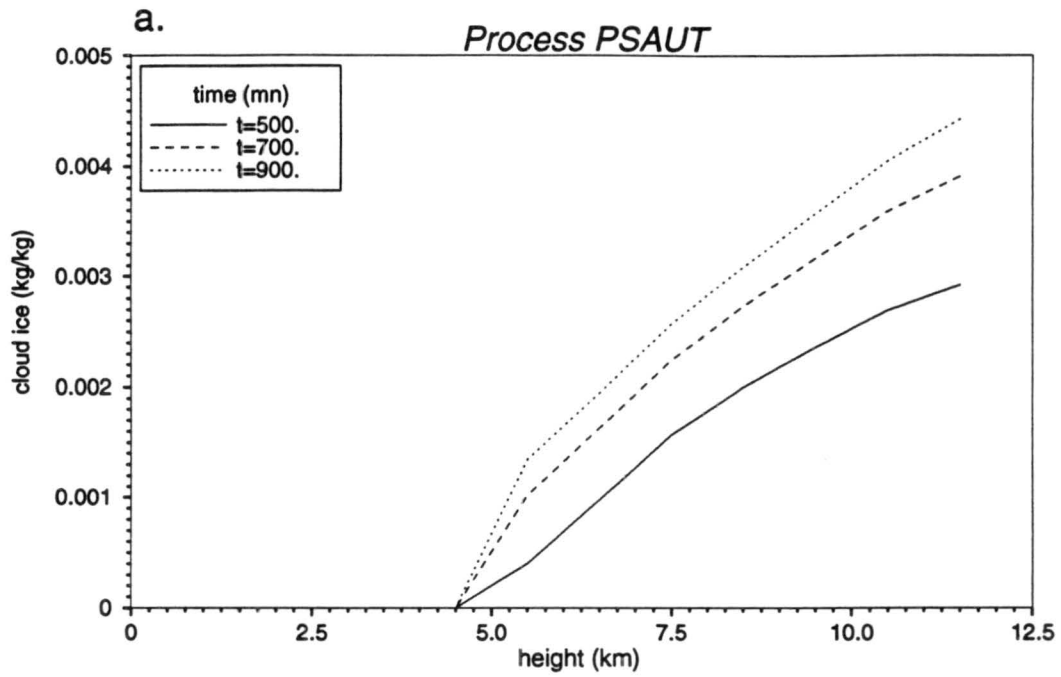


Figure 9: Process PSAUT- Increase of (a) the cloud ice mixing ratio, (b) the snow mixing ratio, and (c) the temperature when supersaturation occurs and snow starts to form by auto-conversion of cloud ice crystals.

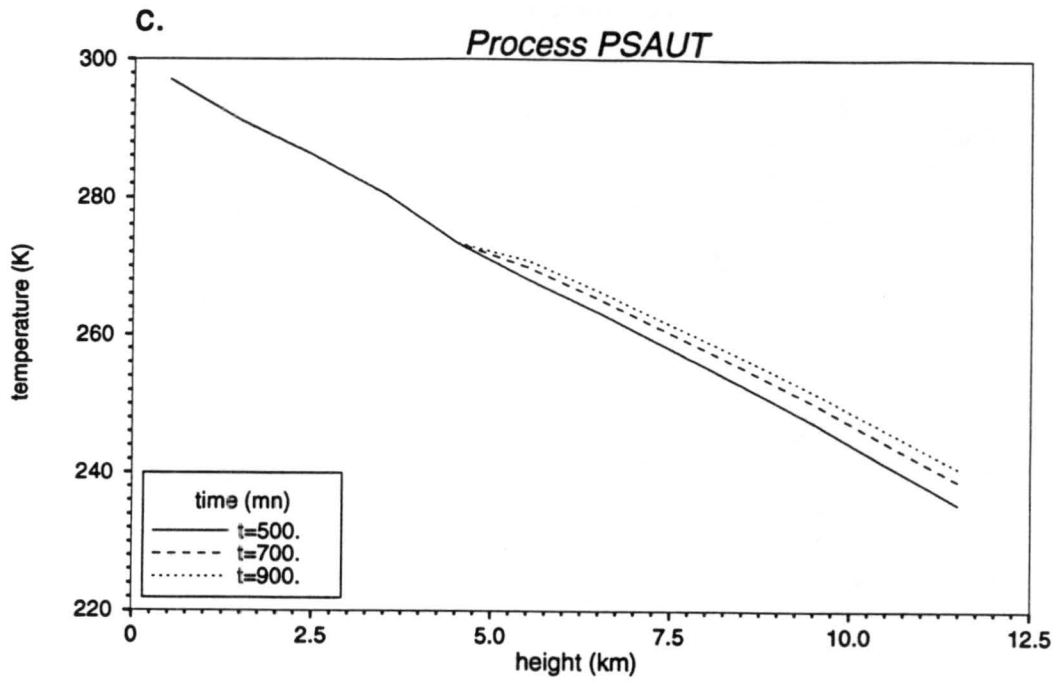


Figure 9: Process PSAUT-continued

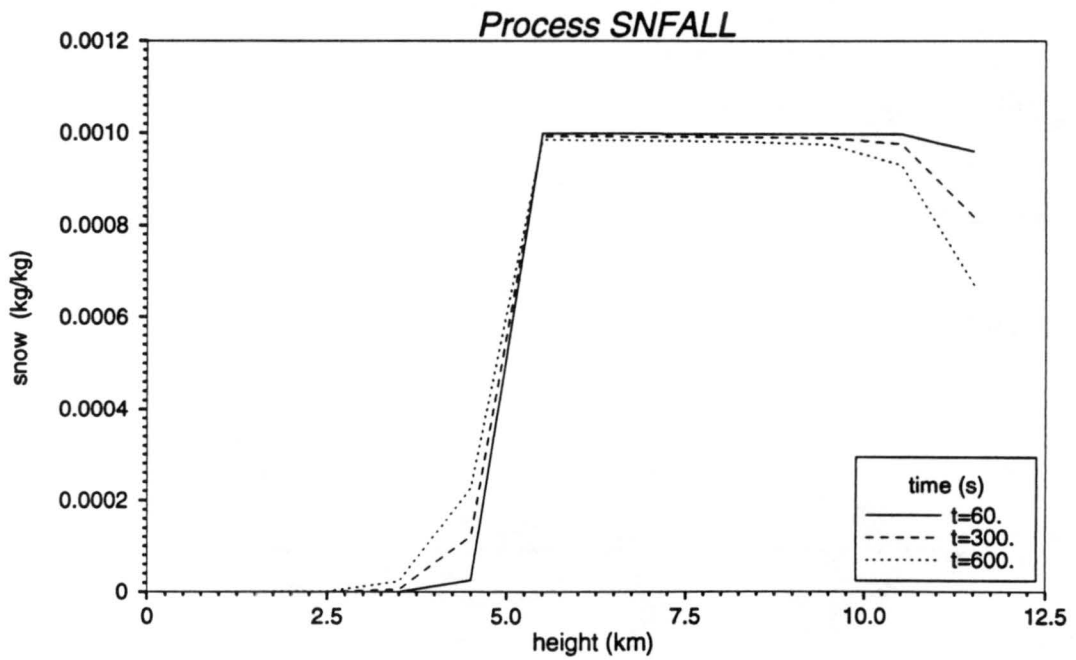


Figure 10: Process SNFALL: Falling of snow.

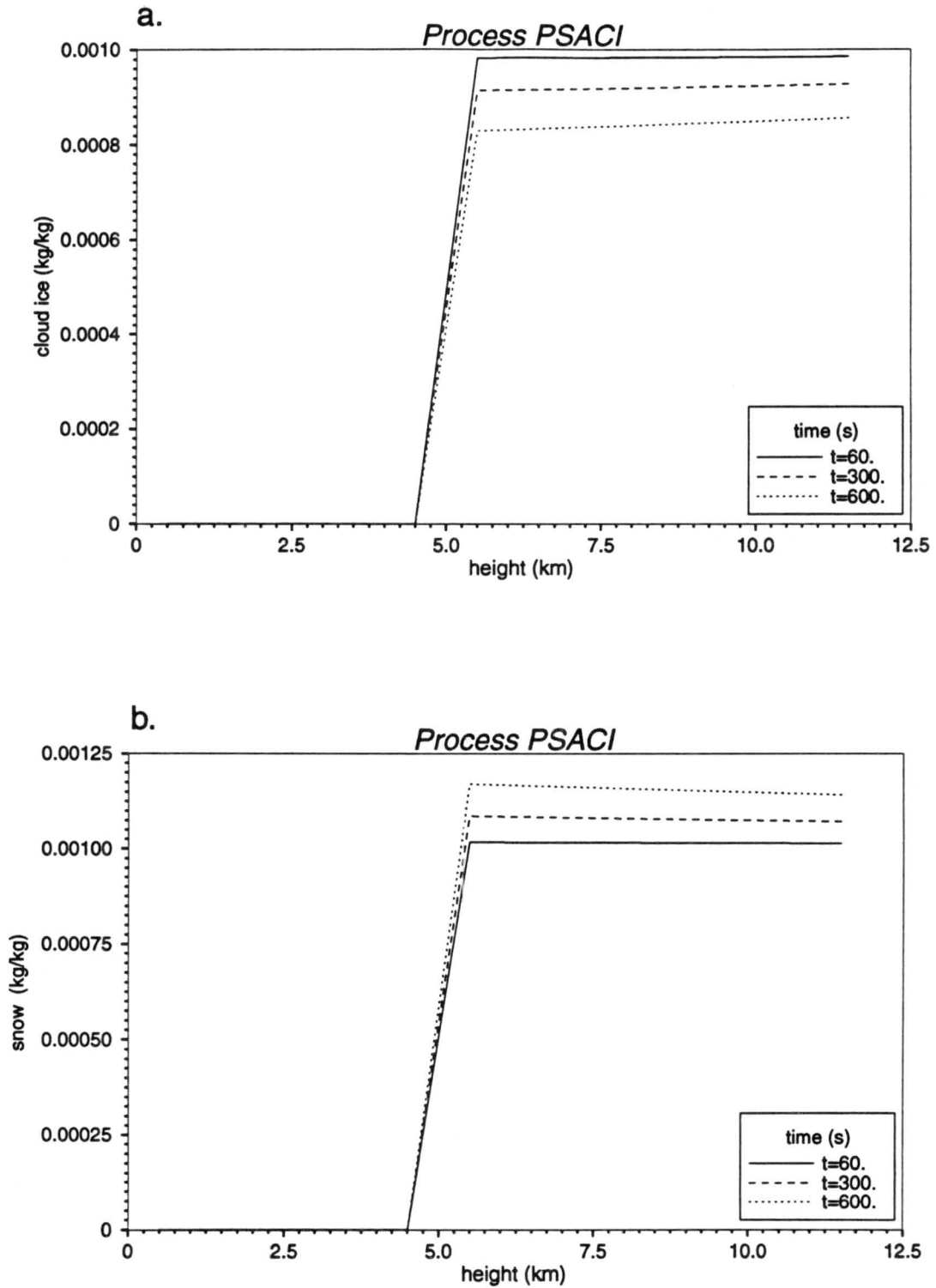


Figure 11: Process PSACI- (a) Decrease of the cloud ice mixing ratio by accretion of snow, and (b) corresponding increase of the snow mixing ratio in layers for which ($T < 0^{\circ}\text{C}$).

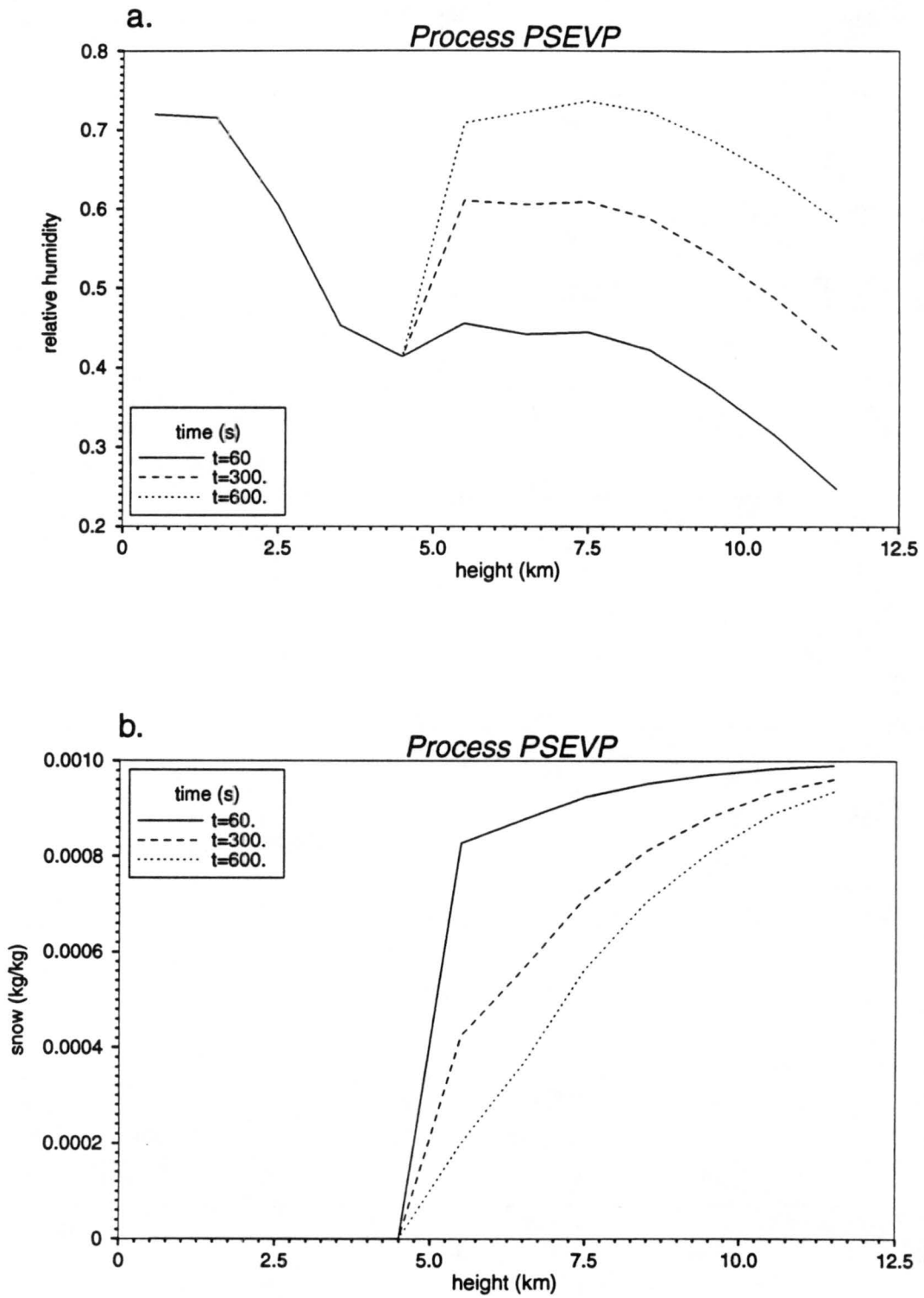


Figure 12: Process PSEVP- (a) Increase of the relative humidity, (b) decrease of the snow mixing ratio, and (c) decrease of the air temperature due to evaporation cooling.

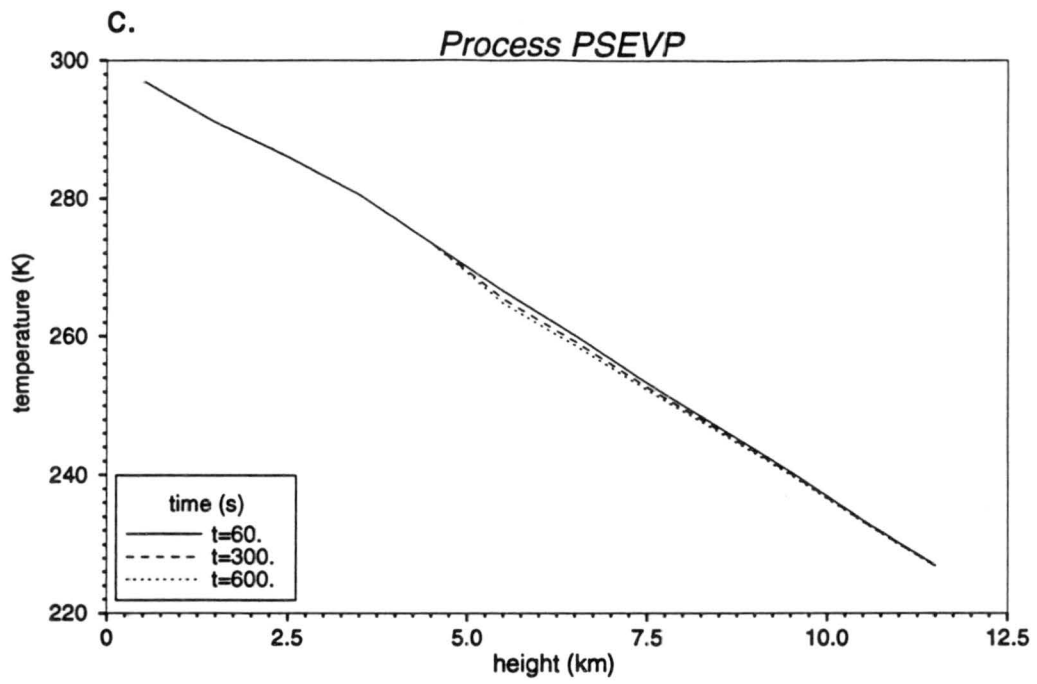


Figure 12: Process PSEVP-continued

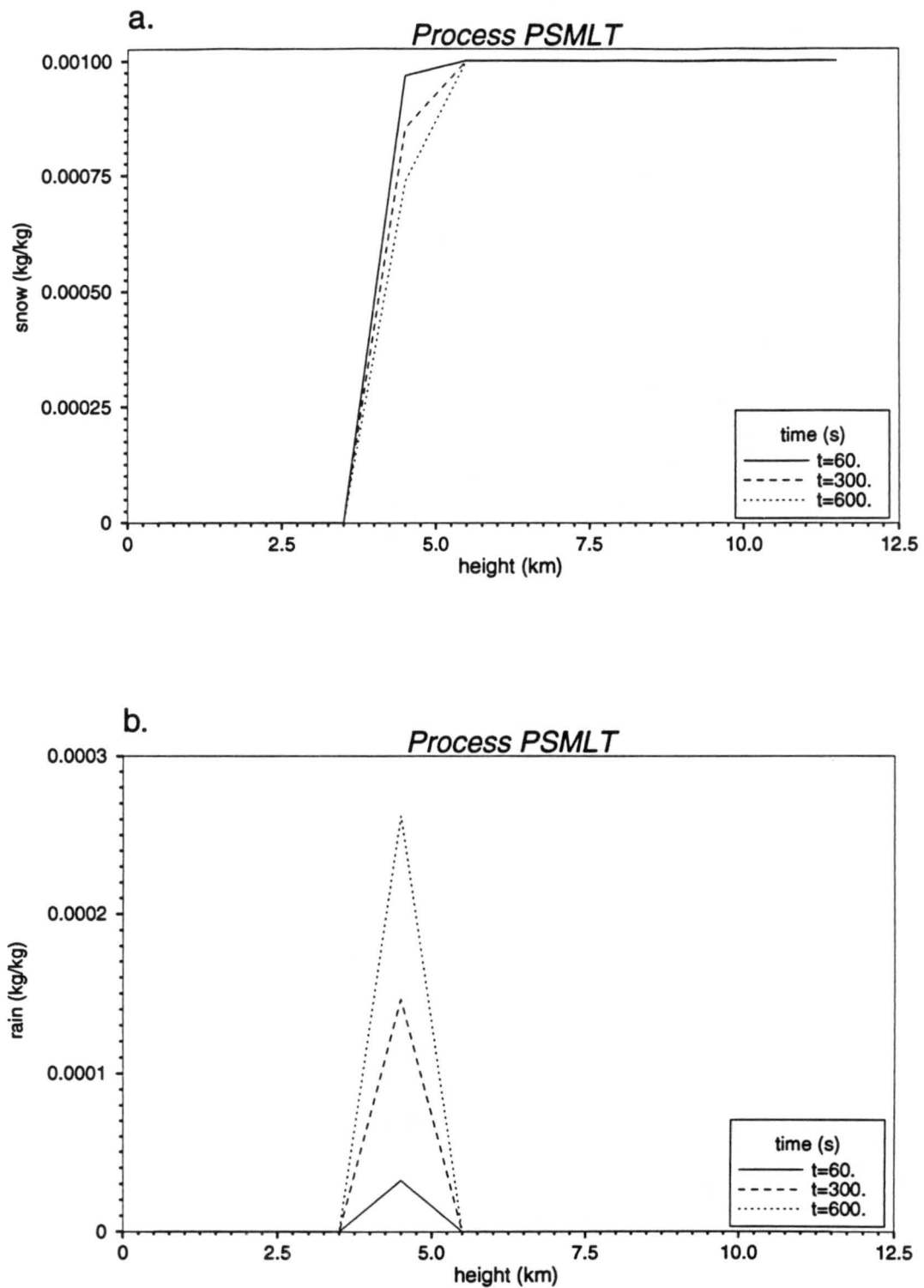


Figure 13: Process PSMLT- (a) Decrease of the snow mixing ratio, and (b) corresponding increase of the rain mixing ratio.

References

- Beard, K.V., and H.R. Pruppacher, 1971: A wind tunnel investigation of the rate of evaporation of small water droplets falling at terminal velocity in air. *J. Atmos. Sci.*, **28**, 1455–1464.
- Byers, H.R., 1965: *Elements of Cloud Physics*. University of Chicago Press, 191 pp.
- Cotton, W.R., M.A. Stephens, T. Nehr Korn, and G.J. Tripoli, 1982: The Colorado State University Three-Dimensional Cloud/Mesoscale Model - 1982. Part II: An ice phase parametrization. *J. Rech. Atmos.*, **16**, 295–320.
- Del Genio, A.D., and M.-S. Yao, 1990: Predicting cloud water variations in the GISS GCM. AMS Conference on Cloud Physics, Preprints Volume, July 23–27, San Francisco, California.
- Flatau, P.J., G.J. Tripoli, J. Verlinde, and W.R. Cotton, 1989: The CSU-RAMS cloud microphysics module. General theory and documentation. Atmos. Sci. Pap. 451, Department of Atmospheric Sciences, Colorado State University, Colorado.
- Ghan, S.J., and R.C. Easter, 1991: Computationally efficient approximations to stratiform cloud microphysics parameterization. *Submitted to J. Geophys. Res.*
- Gunn, K.L.S., and Kinzer, 1949: The terminal velocity of fall for water droplets in stagnant air. *J. Meteor.*, **6**, 243–251.
- Gunn, K.L.S., and J.S. Marshall, 1958: The distribution with size of aggregate snow flakes. *J. Meteor.*, **15**, 452–461.
- Houze, R.A., P.V. Hobbs, P.H. Herzegh, and D.B. Parsons, 1979: Size distributions of precipitation particles in frontal clouds. *J. Atmos. Sci.*, **36**, 156–162.
- Kessler, E., III, 1969: *On the Distribution and Continuity of Water Substance in Atmospheric Circulations*, *Meteor. Monogr.*, No. 32, Amer. Meteor. Soc., 84pp.
- Le Treut, H., and Z.-X. Li, 1991: Sensitivity of an atmospheric general circulation model to prescribed SST changes: feedback effects associated with the simulation of cloud optical properties. *Clim. Dynamics*, **5**, 175–187.
- Lin, Y.-L., R.D. Farley, and H.D. Orville, 1983: Bulk parametrization of the snow field in a cloud model. *J. Climate Appl. Meteor.*, **22**, 1065–1092.
- Locatelli, J.D., and P.V. Hobbs, 1974: Fallspeeds and masses of solid precipitation particles. *J. Geophys. Res.*, **79**, 2185–2197.
- Marshall, J.S., and W. McK. Palmer, 1948: The distribution of raindrops with size. *J. Meteor.*, **5**, 165–166.

- Mason, B.J., 1971: *The Physics of Clouds*. Oxford University Press, 671 pp.
- Mellor, G.L., 1977: The Gaussian cloud model relation. *J. Atmos. Sci.*, **34**, 1483–1484.
- Ose, T. 1991: A prognostic scheme for cirrus clouds in a general circulation model. Ninth Conference on Numerical Weather Prediction, Preprints Volume, October 14–18, Denver, Colorado.
- Pruppacher, H.R., and J.D. Klett, 1978: *Microphysics of Clouds and Precipitation*. D. Reidel, 714 pp.
- Roeckner, E., M. Rieland, and E. Keup, 1990: Modelling of cloud and radiation in the ECHAM model. Proceedings of ECMWF/WCRP Workshop on Clouds, radiative transfer, and the hydrologic cycle, ECMWF, Reading, U.K., 199–222.
- Rutledge, S.A., and P.V. Hobbs, 1983: The mesoscale and microscale structure and organization of cloud bands and precipitation in midlatitude cyclones. VIII: A model for the "Seeder Feeder" process in warm-frontal bands. *J. Atmos. Sci.*, **40**, 1185–1206.
- Smith, R.N.B., 1990: A scheme for predicting layer clouds and their water content in a general circulation model. *Q. J. R. Meteorol. Soc.*, **116**, 435–460.
- Sommeria, G., and J.W. Deardoff, 1977: Sub-grid scale condensation in models of non-precipitating clouds. *J. Atmos. Sci.*, **34**, 344–355.
- Sundqvist, H., 1978: A parameterization scheme for non-convective condensation including prediction of cloud water content. *Q. J. R. Meteorol. Soc.*, **104**, 677–690.
- Sundqvist, H., E. Berger, and J.E. Kristjansson, 1989: Condensation and cloud parameterization studies with a mesoscale numerical weather prediction model. *Mon. Wea. Rev.*, **117**, 1641–1657.
- Thorpe, A.D., and B.J. Mason, 1966: The evaporation of ice spheres and ice crystals. *Brit. J. Appl. Phys.*, **17**, 541–551.
- Weinstein, A.I., 1970: A numerical model of cumulus dynamics and microphysics. *J. Atmos. Sci.*, **27**, 246–255.

A LIST OF SYMBOLS

A.1 Symbols in Section 3

Symbol	Description	Value	SI units
A'	Thermodynamic term in PREVP		m s kg^{-1}
a'	Constant in linear fallspeed relation for rain	3×10^3	s^{-1}
a''	Constant in fallspeed relation for snow	1.139	$\text{m}^{(1-b)} \text{s}^{-1}$
a_0	Coefficient in polynomial fallspeed relation for rain	-0.267	m s^{-1}
a_1	Coefficient in polynomial fallspeed relation for rain	5.15×10^3	s^{-1}
a_2	Coefficient in polynomial fallspeed relation for rain	-1.0225×10^6	$\text{m}^{-1} \text{s}^{-1}$
a_3	Coefficient in polynomial fallspeed relation for rain	7.55×10^7	$\text{m}^{-2} \text{s}^{-1}$
B'	Thermodynamic term in PREVP		m s kg^{-1}
b	Fallspeed exponent for snow	0.11	
C	Capacitance of ice crystal		F
c_p	Specific heat of air at constant pressure	1.005×10^3	$\text{J kg}^{-1} \text{K}^{-1}$
D_R	Raindrop diameter		m
D_S	Snowflake diameter		m
E_r	Evaporation rate		mm day^{-1}
E_{RC}	Rain/cloud water collection efficiency	1	
E_{SC}	Snow/cloud water collection efficiency	1	
E_{SI}	Snow/cloud ice collection efficiency	.1	
e_{si}	Saturation vapor pressure for ice		N m^{-2}
e_{sw}	Saturation vapor pressure for water		N m^{-2}
F	Ventilation factor for rain water		
F'	Ventilation factor for snow		
K_a	Thermal conductivity of air	2.43×10^{-2}	$\text{J m}^{-1} \text{s}^{-1} \text{K}^{-1}$
L_f	Latent heat of fusion of water substance	0.3336×10^6	J kg^{-1}
L_s	Latent heat of sublimation of water substance	2.8336×10^6	J kg^{-1}
L_v	Latent heat of condensation of water substance	2.5×10^6	J kg^{-1}
M_w	Molecular weight of water	18.0160	
$M_{(D_R)}$	Mass of raindrop of diameter D_R		kg
$M_{(D_S)}$	Mass of snowflake of diameter D_S		kg
$N_{D_R dD_R}$	Number concentration of raindrops with diameters between D_R and $D_R + dD_R$		m^{-3}
$N_{D_S dD_S}$	Number concentration of snowflakes with diameters between D_S and $D_S + dD_S$		m^{-3}
N_{0R}	Intercept value in raindrop size distribution	8×10^6	m^{-4}
N_{0S}	Intercept value in snowflake size distribution	2×10^7 (Type 1) 8×10^6 (Type 2)	m^{-4} m^{-4}

LIST OF SYMBOLS (Continued)

Symbol	Description	Value	SI units
n_c	Number concentration of cloud ice crystals		m^{-3}
p_0	Constant in empirical relation	10^5	$N m^{-2}$
p	Pressure		$N m^{-2}$
PCOND	Condensation of water vapor to cloud water/ Evaporation of cloud water to water vapor		$kg kg^{-1} s^{-1}$
PRAUT	Autoconversion of cloud water to rain		$kg kg^{-1} s^{-1}$
PRACW	Collection of cloud droplets by rain		$kg kg^{-1} s^{-1}$
PREVP	Evaporation of rain		$kg kg^{-1} s^{-1}$
PSUB	Sublimation of water vapor to cloud ice/ Evaporation of cloud ice to water vapor		$kg kg^{-1} s^{-1}$
PSAUT	Autoconversion of cloud ice to snow		$kg kg^{-1} s^{-1}$
PSACI	Collection of cloud ice by snow		$kg kg^{-1} s^{-1}$
PSACW	Collection of cloud water by snow; produces snow if $T < T_0$ or rain if $T \geq T_0$. Also enhances snow melting for $T \geq T_0$.		$kg kg^{-1} s^{-1}$
PSEVP	Evaporation of snow		$kg kg^{-1} s^{-1}$
PSMLT	Melting of snow of to form rain, $T \geq T_0$		$kg kg^{-1} s^{-1}$
PSMLTI	Melting of cloud ice to form cloud water, $T \geq T_0$		$kg kg^{-1} s^{-1}$
P_r	Precipitation rate	$mm day^{-1}$	
q_{c0}	Conversion of cloud water to rain threshold		$kg kg^{-1}$
q_c	Mixing ratio of cloud water		$kg kg^{-1}$
q_i	Mixing ratio of cloud ice		$kg kg^{-1}$
q_{i0}	Conversion of cloud ice to snow threshold		$kg kg^{-1}$
q_r	Mixing ratio of rain water		$kg kg^{-1}$
q_s	Mixing ratio of snow		$kg kg^{-1}$
q_{si}	Saturation mixing ratio with respect to ice		$kg kg^{-1}$
q_{sw}	Saturation mixing ratio with respect to water		$kg kg^{-1}$
q_v	Mixing ratio of water vapor		$kg kg^{-1}$
R^*	Universal gas constant	8.314×10^3	$J kmol^{-1} K^{-1}$
R_w	Gas constant for water vapor	4.61×10^2	$J kg^{-1} K^{-1}$
S	Saturation ratio with respect to water		$kg kg^{-1}$
S_C	Source term for cloud water		$kg kg s^{-1}$
S_h	Diabatic heating terms		$K kg kg s^{-1}$
S_I	Source term for cloud ice		$kg kg s^{-1}$
S_i	Saturation ratio with respect to ice		$kg kg s^{-1}$
S_0	Represents sources and sinks for q		$kg kg s^{-1}$
S_R	Source term for rain		$kg kg s^{-1}$
S_S	Source term for snow		$kg kg s^{-1}$
S_V	Source term for water vapor		$kg kg s^{-1}$
T	Temperature		K
T_0	Reference temperature	273.16	K

LIST OF SYMBOLS (Continued)

Symbol	Description	Value	SI units
\bar{V}	Mass-weighted fallspeed of precipitation		m s^{-1}
\bar{V}_R	Mass-weighted fallspeed of rain		m s^{-1}
$V_R(D_R)$	Fallspeed of raindrop of diameter D_R		m s^{-1}
\bar{V}_S	Mass-weighted fallspeed of snow		m s^{-1}
$V_S(D_S)$	Fallspeed of snowflake of diameter D_S		m s^{-1}
α	Rate coefficient for autoconversion (PRAUT)	0.001	s^{-1}
β	Rate coefficient for autoconversion (PSAUT)		s^{-1}
Γ	Gamma function		
ϵ_0	Permittivity of free space	8.854×10^{-12}	
ρ	Air density		kg m^{-3}
ρ_L	Density of water	10^3	kg m^{-3}
ρ_S	Density of snow	100 (Type 1) 200 (Type 2)	kg m^{-3} kg m^{-3}
λ_R	Slope of raindrop size distribution		m^{-1}
λ_S	Slope of snow size distribution		m^{-1}
χ	Diffusivity of water vapor in air	2.26×10^{-5}	$\text{m}^2 \text{s}^{-1}$
μ	Dynamic viscosity of air	1.718×10^{-5}	$\text{kg m}^{-1} \text{s}^{-1}$
Δt	Time increment		s

A.2 Symbols in Section 4

Symbol	Description	Value	SI units
div(qri)	Net change of snow mixing ratio due to falling of snow		$\text{kg kg}^{-1} \text{s}^{-1}$
div(qrw)	Net change of rain mixing ratio due to falling of rain		$\text{kg kg}^{-1} \text{s}^{-1}$
dqci	Change in cloud ice mixing ratio		$\text{kg kg}^{-1} \text{s}^{-1}$
dqcw	Change in cloud water mixing ratio		$\text{kg kg}^{-1} \text{s}^{-1}$
dqri	Change in snow mixing ratio		$\text{kg kg}^{-1} \text{s}^{-1}$
dqrw	Change in rain water mixing ratio		$\text{kg kg}^{-1} \text{s}^{-1}$
qci ₀	Initial mixing ratio of cloud ice		kg kg^{-1}
qci	Final mixing ratio of cloud ice		kg kg^{-1}
qcw ₀	Initial mixing ratio of cloud water		kg kg^{-1}
qcw	Final mixing ratio of cloud water		kg kg^{-1}
qri ₀	Initial mixing ratio of snow		kg kg^{-1}
qri	Final mixing ratio of snow		kg kg^{-1}
qrw ₀	Initial mixing ratio of cloud water		kg kg^{-1}
qrw	Final mixing ratio of rain		kg kg^{-1}
qsati ₀	Initial saturation mixing ratio with respect to ice		kg kg^{-1}
qsati	Final saturation mixing ratio with respect to ice		kg kg^{-1}
qsatw ₀	Initial saturation mixing ratio with respect to water		kg kg^{-1}
qsatw	Final saturation mixing ratio with respect to water		kg kg^{-1}
T ₀	Initial temperature		K
T	Final temperature		K